Self Heating of Sulphide Ores, A Study of Chemical Interaction between Elemental Sulphur and Pyrrhotite

Heekang Kim
Department of Mining and Materials Engineering
McGill University
Montreal, Canada

A thesis submitted to McGill University in partial fulfilment of the requirements of the degree of Master of Science

Abstract

Sulphide minerals are sources of industrial metals such as copper and nickel and precious metals such as gold and silver. During various stages of mineral processing, sulphide minerals are susceptible to Self-Heating (SH), a phenomenon where a material heats up without an external heat source. The detrimental effects of sulphide SH range from minor affects on flotation to major disruptions such as loss of equipment and life. SH is an exothermic oxidation reaction that occurs in three distinct stages, termed Stage A, Stage B, and Stage C. SH reactions are heavily influenced by the interaction between elemental sulphur and sulphide minerals during ambient oxidation reactions. This interaction is affected by many factors, such as time, oxygen content, moisture content, elemental sulphur content and temperature. This thesis focuses on the role of elemental sulphur and its interaction with sulphide minerals. This work employed X-ray Photoelectron Spectroscopy (XPS) to understand their chemical interaction and employed a statistical Design of Experiments (DOE) to investigate how different factors influence their effect on Self-Heating Capacity (SHC). This study found that elemental sulphur created during Stage A does not pose a threat of self-heating on its own, and it needs to form a connection with sulphide minerals. Early works of surface chemistry suggested the formation of polysulphides during Stage A as the potential cause of Stage B self-heating reactions. Additionally, the DOE discovered 5 independent factors that influence the connection between elemental sulphur and sulphide minerals, and determined the optimum

conditions that achieved the highest degree of Stage B SHC. The most optimum condition was found to be 8.5 hr, 95°C, 80 ml air/min, 10 wt.% moisture, and 3 wt.% elemental sulphur.

RÉSUMÉ

Les minéraux sulfures sont les sources de métaux précieux tels que l'or et l'argent, et de métaux industriels tels que le cuivre et le nickel. Au cours des différentes étapes du traitement des minéraux, les minéraux sulfures sont sensibles à l'auto-échauffement, un phénomène où il se réchauffe sans source de chaleur externe. Les dangers de l'auto-échauffement des sulfures vont de l'interruption du travail à la perte d'infrastructures et, dans certains cas, à la perte de vies humaines. L'auto-échauffement est une réaction d'oxydation exothermique qui se déroule en trois étapes distinctes, l'Étape A, l'Étape B et l'Étape C. Les réactions d'auto-échauffement sont fortement influencées par l'interaction entre le soufre élémentaire et minéraux sulfurés, durant température ambiante. Cette interaction est affectée par des nombreux facteurs, tels que la teneur en soufre élémentaire, le temps, la teneur en oxygène, la teneur en humidité et la température. Cette étude se concentre sur le rôle du soufre élémentaire durant l'Étape B et utilise XPS pour comprendre son interaction chemique avec les minéraux sulfures. Cette étude a également utilisé un Plan d'Expériences (Design of experiments en anglais) pour étudier comment les différentes conditions environnementales influencent leur interaction, et leur effet sur la SHC. Cette étude a révélé que le soufre élémentaire créé au cours de l'étape A ne constitue pas une menace d'auto-échauffement soi-même, et qu'il doit former une connexion avec les minéraux sulfurés. Les premiers travaux de chimie de surface ont suggéré la formation de polysulfures au cours de l'étape A comme cause

potentielle des réactions d'auto-échauffement de l'étape B. De plus, le DOE a identifié 5 facteurs indépendants qui influencent la connexion entre le soufre élémentaire et les minéraux sulfurés, et a déterminé les conditions optimales qui ont atteint le plus haut degré de SHC de l'étape B. La condition la plus optimale s'est avérée être 8,5 hr, 95 °C, 80 ml d'air/min, 10 % en poids d'humidité et 3 % en poids de soufre élémentaire.

Acknowledgements

Before I thank everyone that has helped me with this project, I must express my gratitude toward my family. Their unconditional love and support are truly heartwarming, and I hope one day I can do the same.

To Mr. Frank Rosenblum, your knowledge in this field is unparalleled, and your dedication to your craft is an inspiration.

To Dr. Ozan Kokkilic, thank you for all your help with DOE.

To Ray Langlois, for technical training.

To Professor Waters, for supervising and giving me this opportunity.

Table of Contents

List of Figures

List of Tables

Chapter 1 Introduction

1.1 Sulphide Minerals

Sulphide minerals are mineral compounds where sulphur is combined as an anion with a metal cation or cations (Vaughan & Corkhill, 2017). Sulphide minerals are sources of industrial metals such as copper, zinc, and nickel, and precious metals such as gold and silver (Vaughan & Lennie, 1991). A typical sulphide copper deposit contains around 5 wt.% sulphide minerals and 0.7 wt.% copper (Vaughan & Lennie, 1991). With global demand for these metals expected to rise significantly over the next 30 years, more sulphide minerals are to be excavated from the Earth's crust (Yang *et al.*, 2017).

Out of hundreds of discovered sulphides, only five are sufficiently abundant to be categorized as "Rock-Forming" minerals (Deer *et al.*, 1978). The chemical formulas of the Rock-Forming sulphides are displayed in Table 1.1 below.

Table 1.1 "Rock-Forming" sulphide minerals' chemical compositions

Mineral	Chemical Formula
Chalcopyrite	$CuFeS_2$
Galena	PbS
Pyrrhotite	Fe(1-x)S
Pyrite	FeS_2
Sphalerite	Zn(Fe)S

While going through various stages of mineral processing to liberate the desired mineral, sulphide minerals are exposed to a diverse set of environmental conditions. The sulphide

minerals can spontaneously heat up under the right conditions, a process which is commonly referred to as Self-Heating (SH) (Rosenblum & Spira, 1995).

1.2 Self-Heating

Self-Heating (SH) refers to a phenomenon where a material heats up without an external heat source (Rosenblum & Spira, 1995). SH reactions are exothermic in nature, and occur when the rate of heat being generated by the reaction is greater than the rate of heat being dissipated into the surroundings (Ngabe & Finch, 2014).

SH reactions are not unique to sulphide minerals, with cases ranging from powdered milk to coal (Beever & Crowhurst, 1989; Carras & Young, 1994; Nádudvari, 2014). The detrimental effects of SH range from work disruptions, loss of infrastructure, and in some severe cases, loss of life. In Canada, the most notorious cases of sulphide SH related incidents would likely be the mine fires at the Sullivan Mine (British Columbia), and Bathurst Mine (New Brunswick) (Good, 1977; Jung *et al.*, 2020; McCutcheon & Walker, 2019). The Sullivan Mine fire was caused by unattended iron-sulphide extracts, allowing the temperature to reach over 500°C. The Bathurst Mine fire was caused by iron-sulphide backfill, and the fire lasted for more than 25 years.

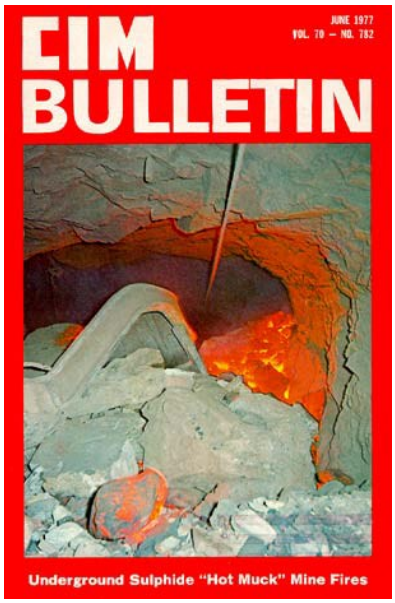

Figure 1.1 Sullivan mine fire - cover page of the CIM Bulletin vol. 70/782, year 1977. Reproduced with permission from (Rosenblum et al., 2001)

Additionally, uncontrolled SH reactions during storage and transportation have led to the sinking of ships, abandonment of cargo and even explosions (Pearse, 1980; Reimers & Hjelmstad, 1987; Yang *et al.*, 2011). Due to these prior accidents, the shipping of most sulphide materials is subjected to the International Maritime Bulk Solids Cargoes Code (IMSBC) (Jung *et al.*, 2020).

Dangers of sulphide SH reactions are not only limited to high temperature, but also the produced off-gas. Sulphide SH reactions release harmful gases (SO_2 and H_2S) and cause oxygen depletion (Rosenblum & Spira, 1995). Sulphur dioxide and hydrogen sulphide are extremely toxic gases, and the dangers range from mild skin irritation to chronic illnesses and even death depending on the exposure (Guidotti, 1996; Legge & Krupa, 2002). SH thus poses logistical and safety challenges at nearly all stages of mineral processing, from mining to concentrate handling and tailings disposal. Therefore, it is critically important to understand the nature of these reactions.

1.3 Thesis Objectives

The objectives of this thesis are:

1. To understand the chemical interaction between elemental sulphur and sulphide minerals during stage B conditions.
2. To evaluate the interactions between factors that influence the interaction between elemental sulphur and sulphide minerals.

1.4. Thesis Structure

This manuscript-based thesis consists of 5 chapters, and presented as the following:

Chapter 1 – Introduction provides the general overview of sulphide minerals, and the Self-Heating phenomenon. The justification of this thesis, and the objectives are also listed in this section.

Chapter 2 – Literature review summarizes all the past work that have been done in this field. This section provides the overview of evaluation tools, mechanisms, factors, and mitigation methods.

Chapter 3 – Manuscript entitled "Role of Elemental Sulphur in Stage B Self-Heating of Sulphide Minerals, and the Potential Role of Polysulphides" presents the research investigating the role of elemental sulphur in Stage B, and its connection with sulphide minerals.

Chapter 4 - Manuscript entitled "Exploring the Connection Between Elemental Sulphur and Sulphide Minerals During Stage A Conditions – a Design of Experiments Investigation" presents the research investigating the numerous factors that influence the interaction between elemental sulphur and sulphide minerals.

Chapter 5 – This chapter summarizes the findings of this thesis and lists the potential future works. The contributions of this thesis to current understandings are also presented.

1.5 Contribution of authors

The manuscript entitled “Role of Elemental Sulphur in Stage B Self-Heating of Sulphide Minerals, and the Potential Role of Polysulphides” (Chapter 3) is co-authored by Prof. K.E. Waters, my supervisor, Dr. O. Kokillic, Research Associate, and Mr. F. Rosenblum as my research co-supervisor. This manuscript was published in the journal “Minerals,” with the following citation.

Kim, Heekang, et al. "Role of Elemental Sulphur in Stage B Self-Heating of Sulphide Minerals, and the Potential Role of Polysulphides." *Minerals* 13.7 (2023): 923.

The manuscript entitled “Exploring the Connection Between Elemental Sulphur and Sulphide Minerals During Stage A Conditions – a Design of Experiments Investigation” (Chapter 4) is co-authored by Prof. K.E. Waters, my supervisor, Dr. O. Kokillic, Research Associate, and Mr. F. Rosenblum as my research co-supervisor. Following the “Sustainable Minerals” conference in June 2023, this manuscript was published in the journal “Minerals Engineering” as a technical note, with the following citation.

Kim, H., et al. "Exploring the Connection Between Elemental Sulphur and Sulphide Minerals During Stage A Conditions–Design of Experiments."

Chapter 2 Literature Review

2.1 Self-Heating Progression

Despite some progress, the sulphide Self-Heating (SH) mechanisms are still not yet fully understood. In the early research, people relied on word of mouth travelling from mine to mine. In the early 1940s for example, one of the proposed theories was that self-heating was caused by wind and the irregular shape of the stockpiles (Rosenblum *et al.*, 2001). As the scope of the research narrowed over the years, it is now known that moisture and oxygen are key components of SH, and the absence of either one will result in no heating (Rosenblum & Spira, 1995).

Based on the current understandings, the sulphide SH reaction progresses in three distinct stages, termed Stage A, Stage B, and Stage C (Rosenblum & Spira, 1995). In each stage, heat is generated by exothermic oxidation reactions, with subsequent stages exhibiting increased heating rate.

Stage A, (also known as the "weathering" stage) occurs in the temperature range between room temperature and 100°C (Rosenblum *et al.*, 2001). In Stage A, a moistened sample oxidizes to create elemental sulphur, a key component for Stage B. In addition to elemental sulphur, sulphur dioxide (SO_2), and hydrogen sulphide (H_2S) are also created (Somot & Finch, 2006).

Following Stage A, Stage B occurs in the temperature range from 100°C to 390°C, where the upper limit varies between minerals (Rosenblum & Spira, 1995). Stage B is a dry reaction since the reaction takes place above the boiling temperature of water (100°C). In Stage B, elemental sulphur formed in Stage A becomes a fuel, and oxidizes to generate more heat and SO_2. The SH reactions occurring in Stage B are dependent on the weathering reactions of Stage A (Rosenblum & Spira, 1995).

Stage C (also known as the “roasting” or “ignition” stage) occurs when the temperature reaches higher than 390°C. At this stage, both reacted and previously un-reacted sulphides from previous stages oxidize to generate heat. Unlike Stage B, Stage C is not dependent on the reaction products from the preceding stages. Figure 2.1 below shows the simplified progression of sulphide SH reactions from Stage A to Stage C.

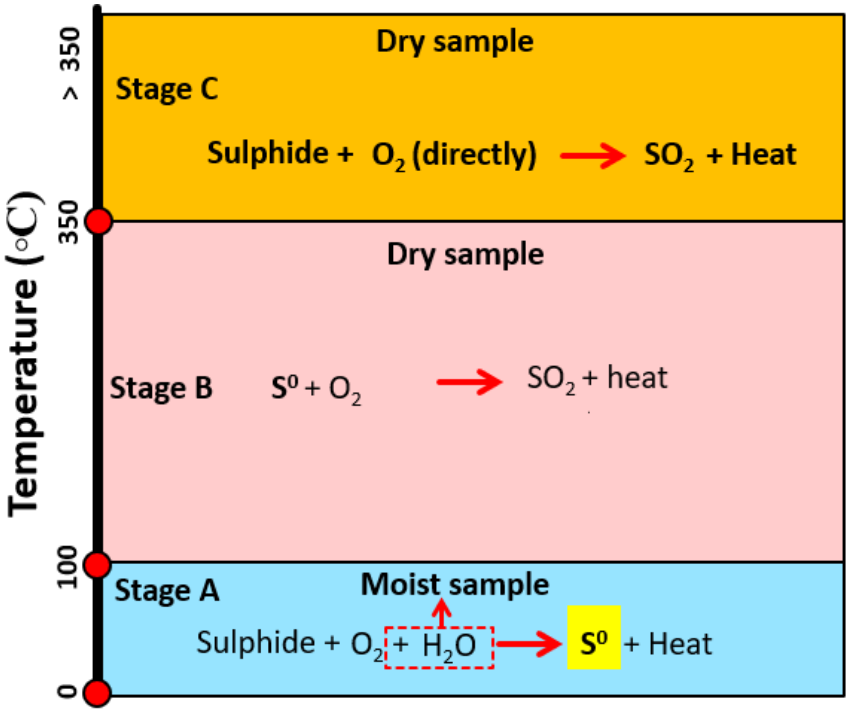

Figure 2.1 Proposed SH progression chart. Adapted from (Moon et al., 2019)

2.2 Self-Heating Measurements

The SH measurement technologies have evolved over time. Since SH reactions pose a threat in nearly all stages of mining activity (excavation, processing, and transportation), the biggest challenge is to predict the SH behavior over time and in situ (Rosenblum *et al.*, 2014). Historically, the SH tests employed a method called a “snapshot test”, where tests were conducted at specific times and conditions. These tests were problematic as they only provided reliable results for invariable materials, i.e. does not change their response over time (Rosenblum *et al.*, 2014).

Table 2.1 below summarizes SH measurement methodologies that are currently employed by the industry. However, Moon *et al.* (2019) highlighted that these methodologies are not always interchangeable, as different methodologies can provide conflicting assessments. The two methodologies that were used to highlight this discrepancy were the United Nations (U.N.) recommended test, and the FR test. This thesis therefore focuses on the two methodologies. However, the reader is referred to Rosenblum *et al.* (2014) where other self-heating measurement methodologies are described in detail.

Table 2.1 Common SH measurement methodologies. Adapted from (Rosenblum et al., 2014)

Stage	Name
Stage A Testing	Dewar Calorimetry
	R_{70} Test
Stage B Testing	Basket Testing Method
	Oxidation Kinetics Testing Method
	F-K
	United Nations (UN) Recommended Test
	Crossing Point Temperature
	Heat Release Method
	Olpinski Index Method
	Activation Energy Method
	Differential Thermal Analysis
	Power Compensated Differential Scanning Calorimetry
	Heat Flux Differential Scanning Calorimetry
Extended Temperature testing (Stage A -> Stage B)	Accelerating Rate Calorimeter
	FR test method
Stage C Testing	DTA/DSC

2.2.1 U.N. Recommended Test

To address the rising concerns involving SH reactions, the U.N. published the first version of the Recommendation on Transport of Dangerous Goods (RTDG) in 1956 (Tanackov *et al.*, 2018; United.Nations, 2011). This document was designed as a guideline for governing bodies, by grouping potentially hazardous materials into separate categories and providing adequate testing methods for evaluation. According to this U.N. publication, flammable solids that are

susceptible to spontaneous combustion when in contact with water belongs to Class 4, which has 3 subdivisions (Tanackov *et al.*, 2018; United.Nations, 2011).

Division 4.1 - Flammable solids and self-reactive substances
Division 4.2 - pyrophoric solids, pyrophoric liquids, and self-heating substances
Division 4.3 - substances that emits flammable gases.

Sulphide minerals fall under Division 4.2 and are categorized as materials that ignite when in contact with air and moisture after long periods of time (hours or days). To evaluate the potential hazards of the sulphide minerals, the U.N. recommends a derivation of the basket test method. This test uses powdered sulphide samples that are gently packed into a $100mm^3$ open-top metal basket (0.05mm mesh) which is placed in an oven for 24 hours at 140°C. Fresh oxygen is supplied constantly throughout the experiment, and the temperature is measured simultaneously by two thermocouples, one placed in the middle of the sample and the other placed in the oven wall (Moon *et al.*, 2019). The schematic of this test apparatus is displayed in Figure 2.2, below.

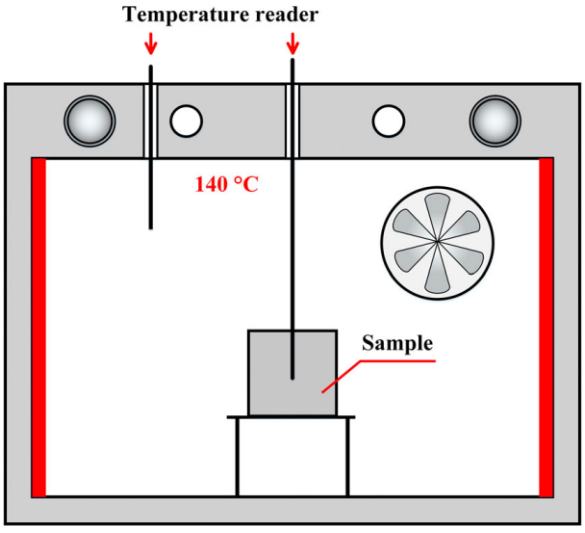

Figure 2.2 U.N recommended test apparatus. Reproduced with permission from (Moon et al., 2019)

If the temperature of the sample surpasses 200°C within 24 hours, the test is deemed to have yielded a "positive result," meaning the sample poses a threat of self heating. The samples that

produced a positive result are subjected to a repeat test with a smaller volume (25mm^3) to further classify the material. If the repeat test also produces a temperature rise above 200°C within 24 hours, the sample is classified as Packing Group II. If the temperature of the repeat sample fails to surpass 200°C within 24 hours, the sample is classified as Packing Group III. The flow chart of the experiment is displayed in Figure 2.3 Below. The U.N. regulations and requirements are currently used by the U.S. Department of transportation (DOT) and Transport Canada (Moon *et al.*, 2019; Tanackov *et al.*, 2018).

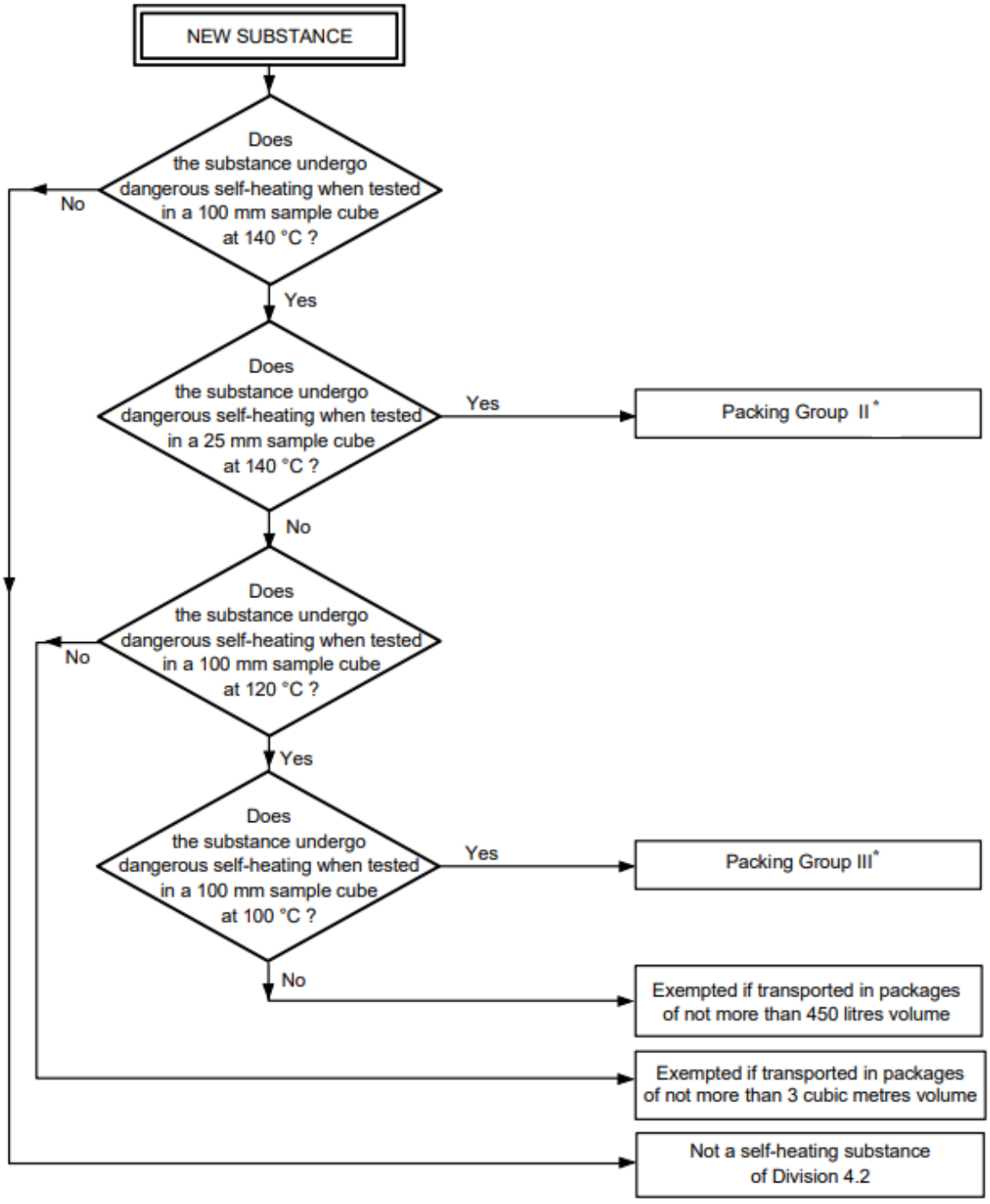

Figure 2.3 U.N test flow chart. Adapted from (United.Nations, 2011)

2.2.2 FR Test

The first version of the FR test was developed in 1982 at Noranda Technology Centre by Rosenblum and Spira (Rosenblum & Spira, 1995). This apparatus was specifically designed to measure Sulphide SH reactions, and upon further improvements in 1995 and 2001, it is now

located in the Department of Mining and Materials Engineering at McGill University. Except for the new gas inlet/outlet system, the apparatus is identical to a calorimeter. The apparatus consists of 5 major components, a 2L Pyrex Vessel, a constant-temperature coiled heater, a metal mesh screen, a concrete base, and an insulator. The schematic of this apparatus is shown in Figure 2.4 below.

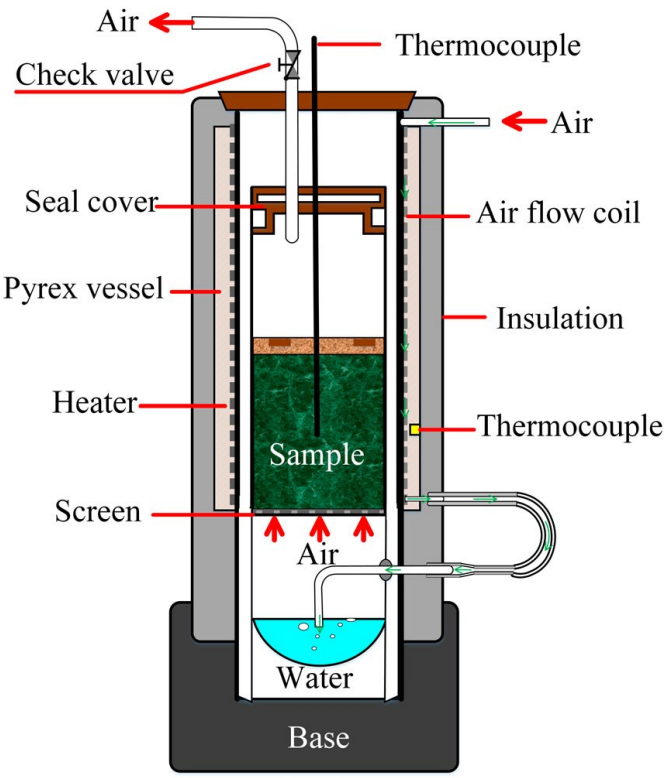

Figure 2.4 FR test apparatus. Reproduced with permission from (Moon et al., 2019)

The test proceeds in two stages, stage A at 70°C followed by stage B at 140 °C. After moistening a granulated 250g sample with 15g of purified (Reverse Osmosis) water, the sample is placed in the 2L Pyrex Vessel. Stage A testing begins by heated up the sample to 70°C with the coiled heater. Once the sample has reached the equilibrium temperature, 100 ml/min of air is injected for 15-minutes every 5 hours for a total of 10 cycles (Rosenblum *et al.*, 2001). This stage serves as an accelerated weathering (oxidation) stage, by supplying both oxygen and water at elevated

ambient temperature. The sample temperature is logged every minute by the thermocouple, while the temperature o the Pyrex Vessel is maintained at 70°C. After the 10^{th} cycle, Stage B testing begins by injecting 250 ml/min of Nitrogen continuously to heat up the temperature to 140°C. Once the sample temperature has again equilibrated, the 15-minute 100ml/min of air injection cycle is repeated for another 10 cycles (Rosenblum *et al.*, 2001).

The thermocouple is connected to a software that graphs the temperature change over time, where the distinction between the reactive (exhibits SH) and non-reactive (does not exhibit SH) samples can be visualized. A reactive sample demonstrates a temperature increase with air injections, whereas a non-reactive sample shows no temperature change. Figure 2.5 below shows the thermograms of reactive and non-reactive samples.

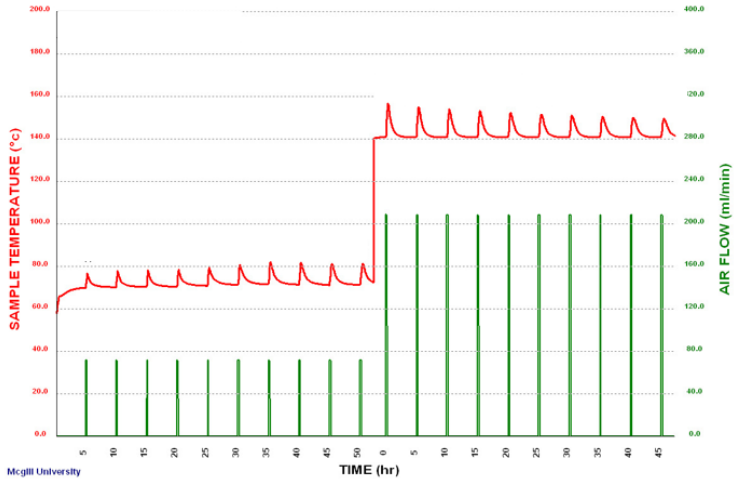

a)

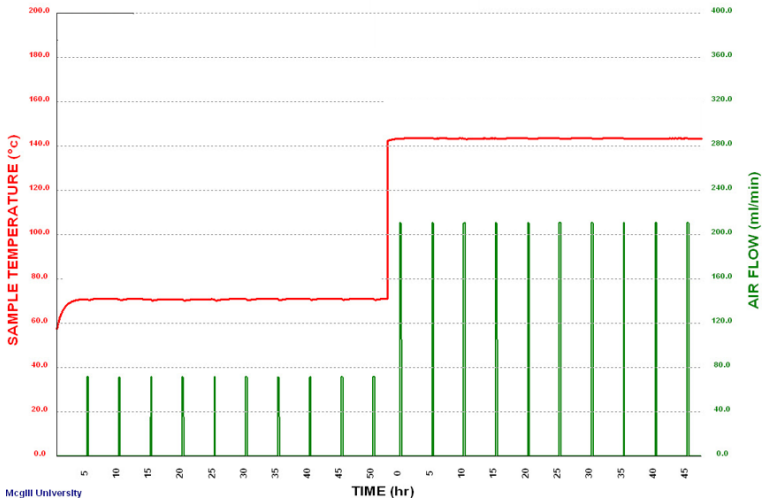

b)

Figure 2.5 a) Thermogram of a reactive sample and b) Thermogram of a non-reactive sample

Using the temperature peaks, the Self-Heating Capacity (SHC) of the reactive samples are calculated with the following equation.

$$SHC_{\,i} = \sum SHR_{\,i} * Cp * t \qquad (2.1)$$

Where: *SHC = Self Heating Capacity (J/g)*
SHR = Self Heating Rate (°C/hr)
*Cp = Specific Heat Capacity (J/g * °C)*
T = Time (hr)

The Self Heating Rate (SHR) at the time of each air injection corresponds with the slope of the temperature peak. Additionally, Rosenblum found that the specific heat values of nearly all the sulphides relevant to this work fall into the range from 0.5 J/g°C to 0.7 J/g°C over the temperature range from 25°C to 500°C (Rosenblum & Spira, 1995). Therefore, A single value of 0.6 J/g°C can be used for all sulphide SHC calculations. As the oxygen-exposure time was capped at 15-minutes, the time (T) can be substituted with the value 0.25.

Therefore, Equation 2.1 can be rewritten as:

$$SHC_{\,i} = \sum SHR_{\,i} * 0.6\left(\frac{J}{g°C}\right) * 0.25hr \tag{2.2}$$

Which can be simplified:

$$SHC_{\,i} = \sum SHR_{\,i} * 0.15 \tag{2.3}$$

With these measurements, Rosenblum *et al*. (1995) created a risk assessment chart that quantifies the potential hazard of the sulphide sample. By putting the SHC of the sample in stage A on the x-axis and SHC of the sample in stage B on the y-axis, the risk assessment chart classifies material into five regions. Region 1, where material is deemed safe and there is no threat of SH (Rosenblum & Spira, 1995). Region 2, where material will experience some SH, but will not go over 100°C. Region 3, where material has potential of high SH, therefore should be kept away from high heat sources. Region 4, where material is likely to undergo SH, therefore constant monitoring is required. Lastly Region 5 where the material will undoubtably undergo SH, therefore prevention actions are required. The risk assessment is shown in Figure 2.6 below.

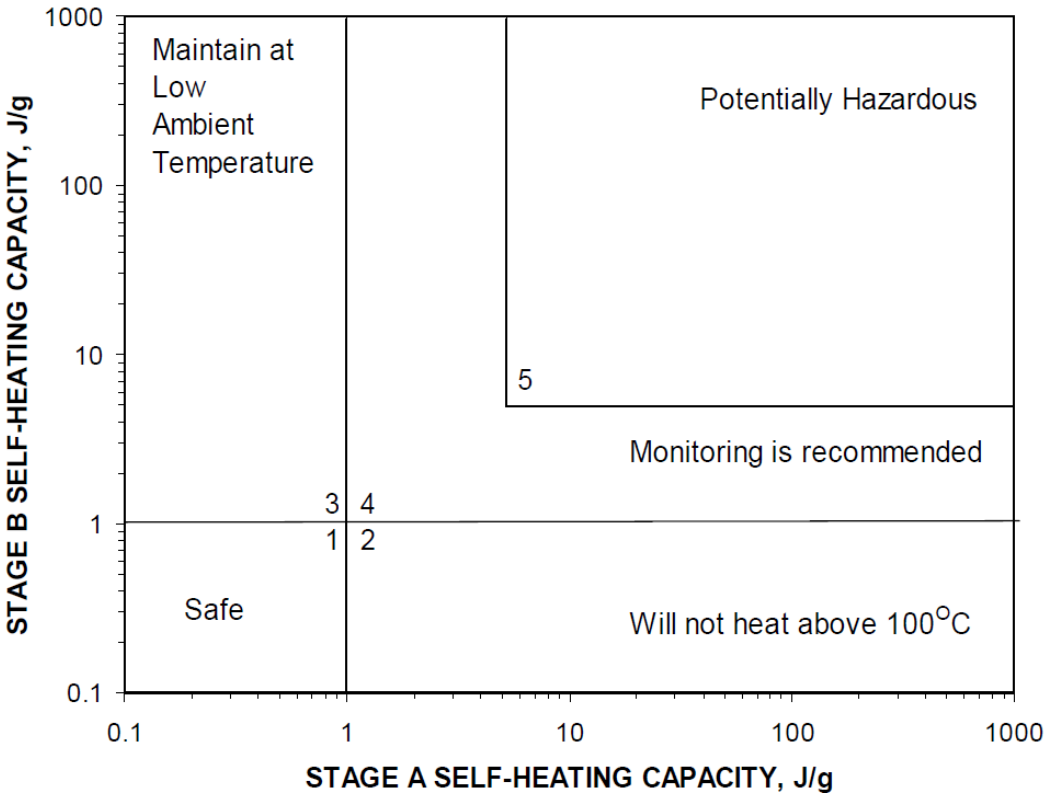

Figure 2.6 Risk assessment chart. Reproduced with permission from (Payant et al., 2012)

2.2.3 Comparison

Moon *et al.* (2019) took two identical sulphide samples, and subjected one to the UN recommended test, and the other to the FR test. The U.N. test deemed the material safe, whereas the FR test classified the material into region 5, recommending preventative actions. This false negative was caused by the difference in testing methods. The U.N. test is a single stage test that does not consider the effects of oxidation reactions at ambient temperatures (weathering). On the other hand, the FR test employees a two-stage test. In effect, the U.N. test only considers the Stage B equivalent of the FR test (exposure to oxygen at 140°C).

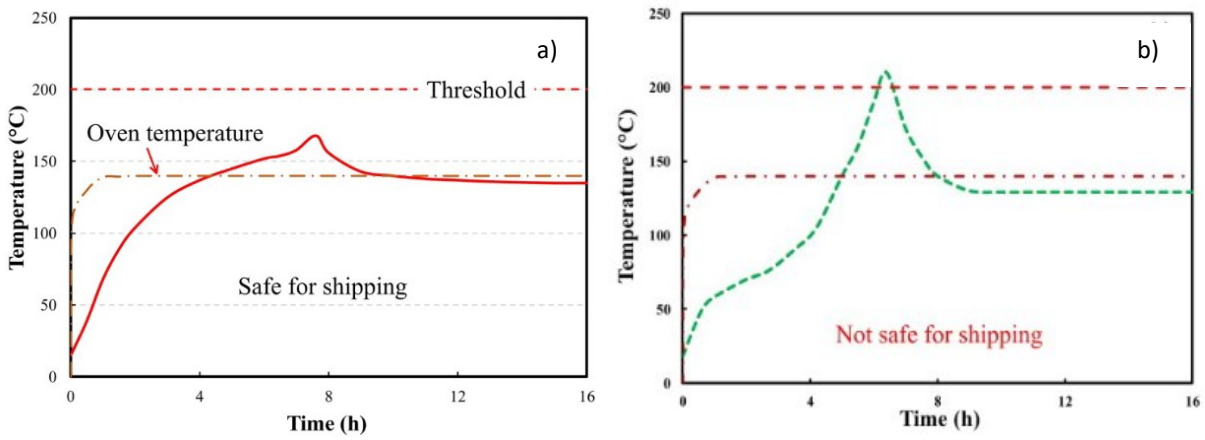

Figure 2.7 a) U.N. test of As-received sample and b) U.N test of sample after weathering stage. Reproduced with permission from (Moon et al., 2019)

The shortcoming of single stage testing is visualized in Figure 2.7 above. This discrepancy is related to the sequence of sulphide oxidation. As mentioned previously, the weathering stage creates elemental sulphur, which fuels Stage B reactions. Therefore, a weathering stage must be simulated in any test protocol assessing the SH potential of sulphides (Moon *et al.*, 2019).

2.3 Weathering Apparatus

The weathering stage (Stage A) is where moist sulphide minerals undergo oxidation reactions in ambient temperatures. To simulate this occurrence, the FR test uses accelerated weathering conditions for stage A (50 hours at 70°C) (Rosenblum *et al.*, 2015). Although this suits the needs of a rapid standardized test, it does not scale well to specific field conditions. Therefore, Rosenblum *et al.* (2015) developed a weathering apparatus to investigate the effects of varying field conditions that might differ from the standardized test conditions. The weathering apparatus consists of 5 main parts, a sealed test chamber, an off-gas analyzer, a relative humidity (RH) probe, a thermocouple and three gas ports. Air (moist or dry) or nitrogen or a combination of both is used to control the oxidation reaction, and the exhaust is dried and sent to a gas analyzer (Rosenblum *et al.*, 2015). This schematic diagram is shown in Figure 2.8 below.

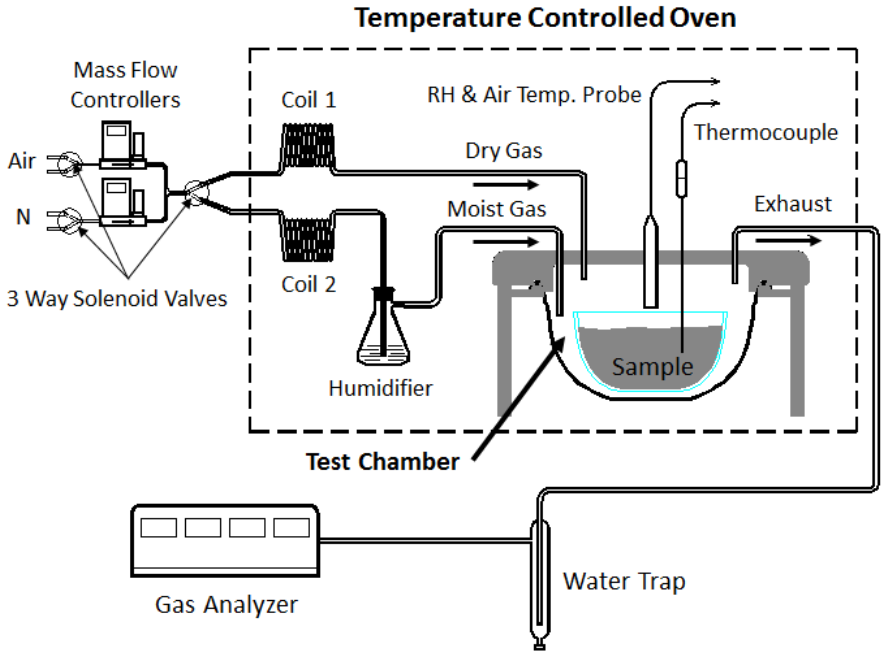

Figure 2.8 Weathering apparatus. Reproduced with permission from (Rosenblum et al., 2015)

2.4 Factors Effecting Self-Heating.

2.4.1 Elemental Sulphur

The crucial role of elemental sulphur during SH reactions has been well documented by Rosenblum *et al.* (1995). Using the FR test, they observed the sulphur content increasing from practically 0 wt.% to over 3 wt.% during the Stage A test period (conducted for 50h at 70°C) and decreasing from 3 wt.% to 0 wt.% in Stage B (50 hours at 140°C) (Rosenblum & Spira, 1995). It is important to note that when the elemental sulphur was reduced to 0 wt.% in Stage B, the heating stopped. This experiment is visualized in Figure 2.9 below.

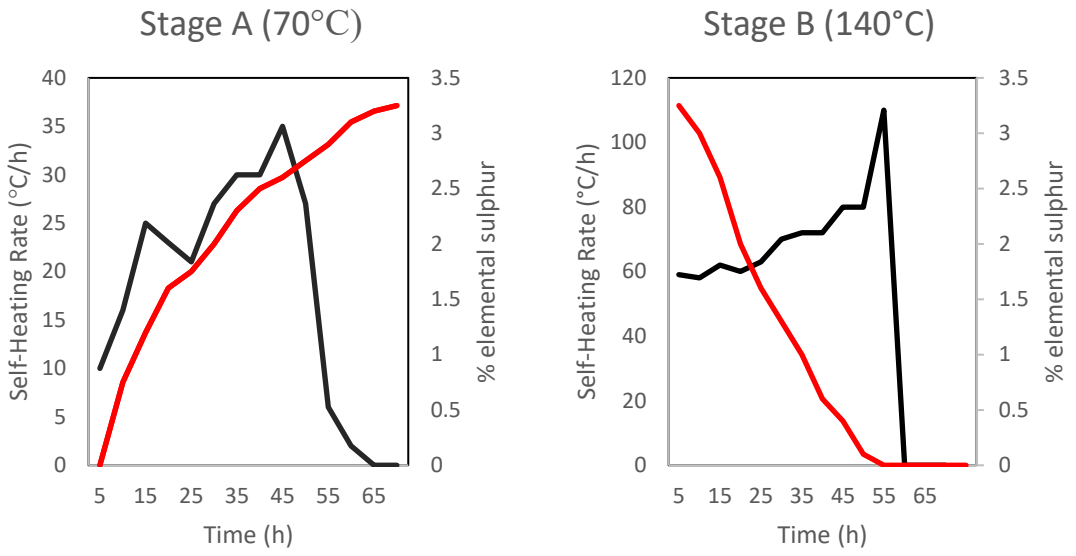

Figure 2.9 Elemental sulphur generation and oxidation. Adapted from (Rosenblum & Spira, 1995)

The creation of elemental sulphur during weathering stage can be examined visually, and it has been spotted in both laboratory settings, and in the field (Rosenblum *et al.*, 2014).

a)

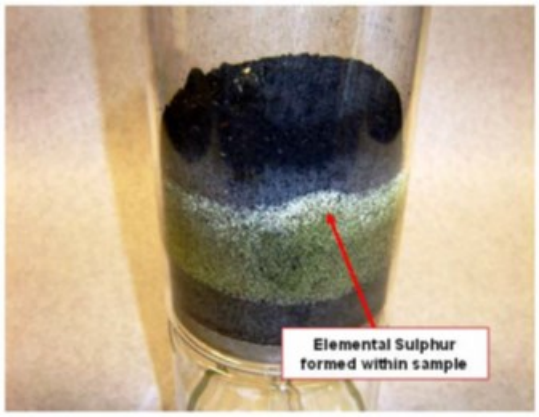

b)

Figure 2.10 a) Pyrex cell of FR test and b) elemental sulfur found in the mine site. Reproduced with permission from (Rosenblum et al., 2014)

The link between the elemental sulphur weight content and the resulting SHC was further emphasized when nickel concentrates caught fire while they were being transported from an Australian mine to a Canadian smelter (Rosenblum *et al.*, 2014). To analyze the cause of this fire,

samples were subsequently taken along the route and analyzed for elemental sulphur content. The samples were subjected to Stage B of the FR test to see the SHC of each sample, and their results are shown in Figure 2.11 below.

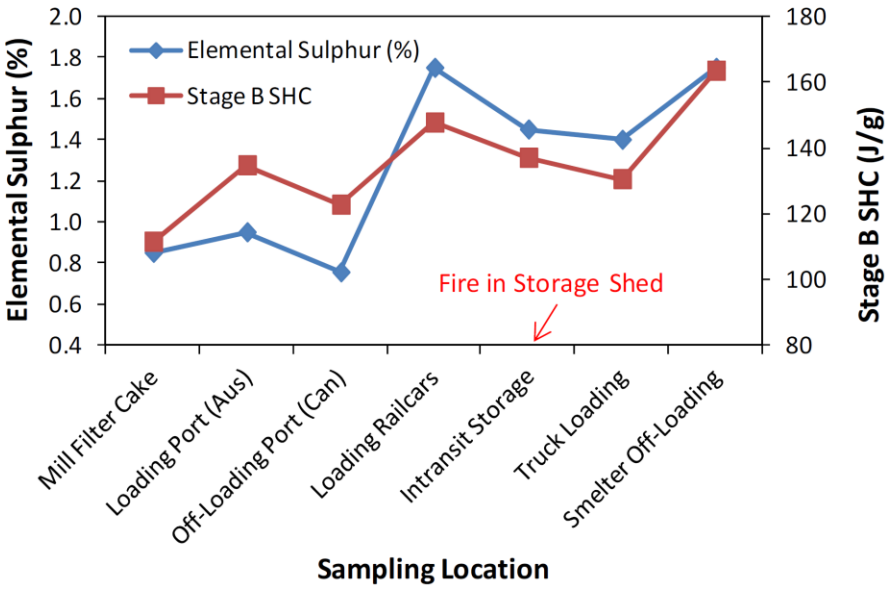

Figure 2.11 Evolution of elemental sulphur. Reproduced with permission from (Rosenblum et al., 2014)

Figure 2.11 shows the elemental sulphur content more than doubling from the point of origin at the mine to off-loading at the smelter. As the elemental sulphur weight content increased, the SHC increased from 100 J/g to 160 J/g accordingly (Rosenblum *et al.*, 2014).

2.4.2 Weathering Time

Using the weathering apparatus described in Section 2.3, Rosenblum *et al.* (2015) showed the proportional relationship between weathering time and SHC. A set of nickel concentrates were exposed to varying degrees of weathering time (7 days to 21) then sent for Stage B testing (Rosenblum *et al.*, 2015). The experimental result shown in Figure 2.12 below demonstrates that after an initial delay of approximately 7 days, the SHC increased with weathering time. After 14 days, the SHC rose to 23.8 J/g, and after 21 days to 50.8 J/g (Rosenblum *et al.*, 2015).

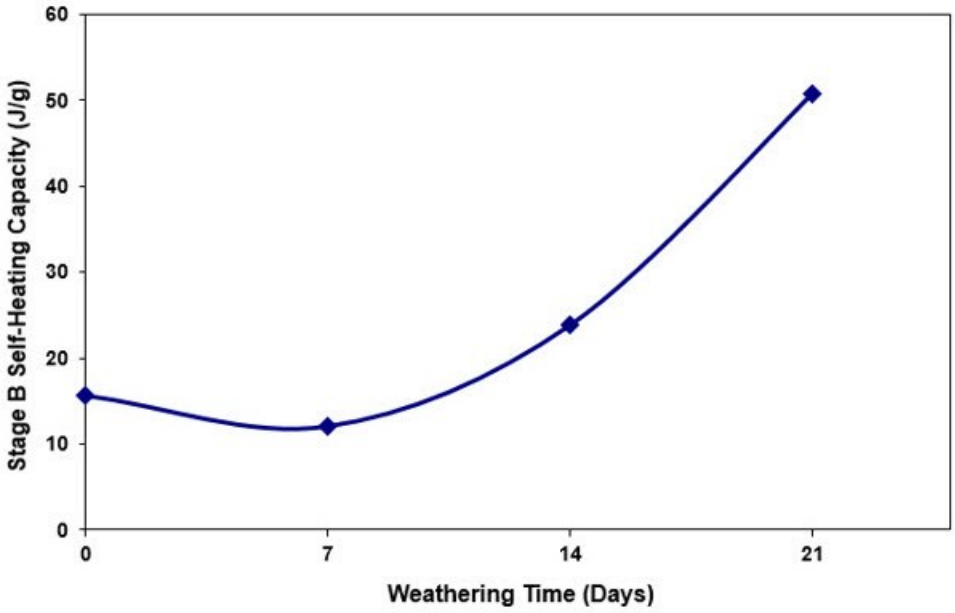

Figure 2.12 Weathering time vs SHC. Reproduced with permission from (Rosenblum et al., 2015)

2.4.3 Ambient Humidity

Using the weathering apparatus mentioned in Section 2.3, Rosenblum *et al.* (2015) showed the proportional relationship between ambient humidity during weathering and SHC. Two sets (one wet, one dry) active nickel concentrate samples with varying degrees of ambient humidity (30%, 50%, 70%, and 85%) were weathered for 21 days at 40 °C before being subjected to Stage B testing (Rosenblum *et al.*, 2015). Test results shown in Figure 2.13 below demonstrate that the dry sample showed no increase in Stage B SHC until the ambient humidity increased above 70%. The wet samples consistently demonstrated higher SHC values than the dried samples and responded to increase in RH in a similar but more dramatic fashion. The SHC rose from 18.1 J/g at 70% RH, to 60.7 J/g at 85% RH (Rosenblum *et al.*, 2015).

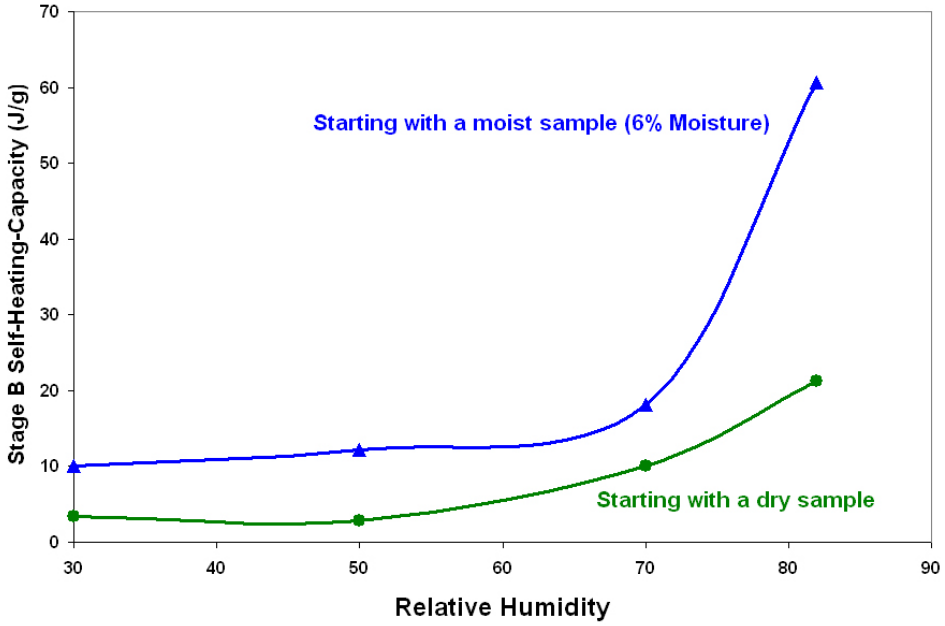

Figure 2.13 Relative humidity vs SHC. Reproduced with permission from (Rosenblum et al., 2015)

2.4.4 Oxygen Content in Air

Using the same weathering apparatus, Rosenblum tested the effect of oxygen content during weathering on SHC. One set of dry samples and another set of moist samples were weathered for 21 days at 80% RH and 40°C temperature with varying degrees of oxygen content before being subjected to stage B testing (Rosenblum *et al.*, 2015).

The results shown in Figure 2.14 below reinforce the importance of oxygen as no SH was observed from samples that lacked access to oxygen. The SHC steadily increased with increasing oxygen content and peaked at ~5% oxygen for both sets of samples. Similar to Section 2.4.3, the moist sample had significantly higher SHC values in all data points. As the oxygen content increases beyond 5%, the SHC began to tail off, dropping to almost half of the peak SHC value (Rosenblum *et al.*, 2015).

Although the tail-off is not yet fully understood, Rosenblum *et al.* (2015) postulated that a higher oxygen content caused a more complete oxidation of the sulphides, which led to the formation of sulphates and/or hydroxy-sulphates. This result may help to explain what has been observed in the field; that the maximum temperature in a pile will occur 30 to 50 cm below the surface, where oxygen content and heat dissipation rate is lower than at or near the surface (Rosenblum *et al.*, 2015).

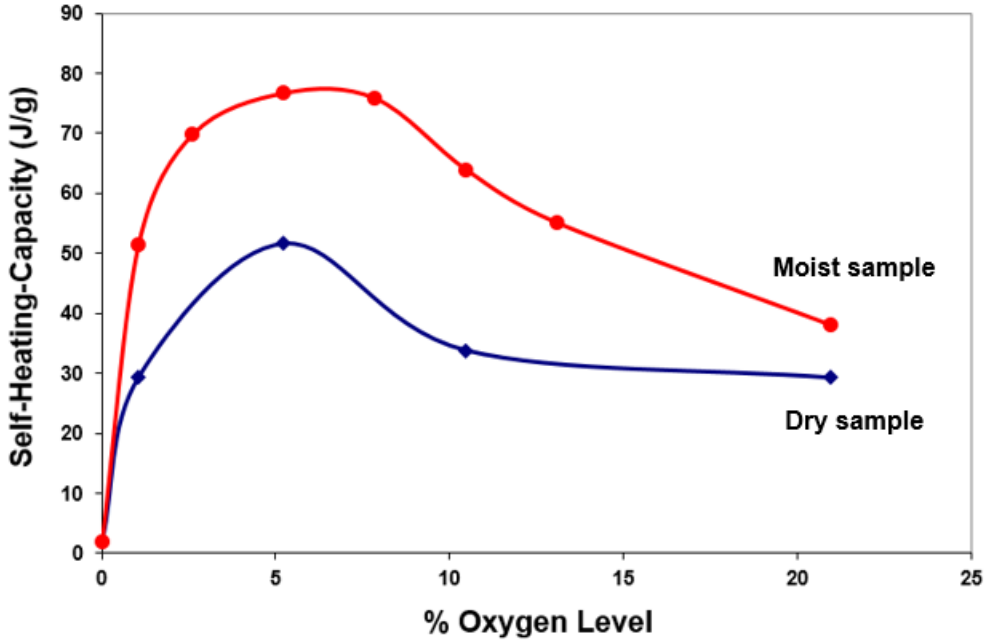

Figure 2.14 Affect of oxygen content on stage B SHC. Reproduced with permission from (Rosenblum et al., 2015)

2.4.5 Moisture

It was noted in the previous sections (2.4.3, 2.4.4) that moist samples exhibited a much higher SHC than dry samples. This is due to the strong interactive nature between moisture, humidity, and oxygen. The moisture content of the material continuously changes due to evaporation and consumption by oxidation reactions. Humidity replenishes water to the sulphide minerals, allowing weathering to continue even above evaporation temperatures. The past studies have

shown that this interaction is especially critical during the first few hours of the test, where it governs the driving force to sustain the oxidation reaction in Stage A (Payant *et al.*, 2012; Rosenblum *et al.*, 2001; Rosenblum *et al.*, 2014; Rosenblum & Spira, 1995). Figure 2.15 below shows the link between moisture with SHR and O_2 consumption rate. The study shows that the SHC peaked at the moisture content of 4 wt.% and decreased linearly as moisture increases. This decline is caused by the energy being used to raise the temperature of the excess water in the system rather than raising the temperature of the sample. This phenomenon is known as "water flooding," and it is one of the common mitigation methods (Rosenblum *et al.*, 2001). Therefore, to completely prevent SH, it is recommended to store sulphide minerals either underwater, or in bone-dry conditions.

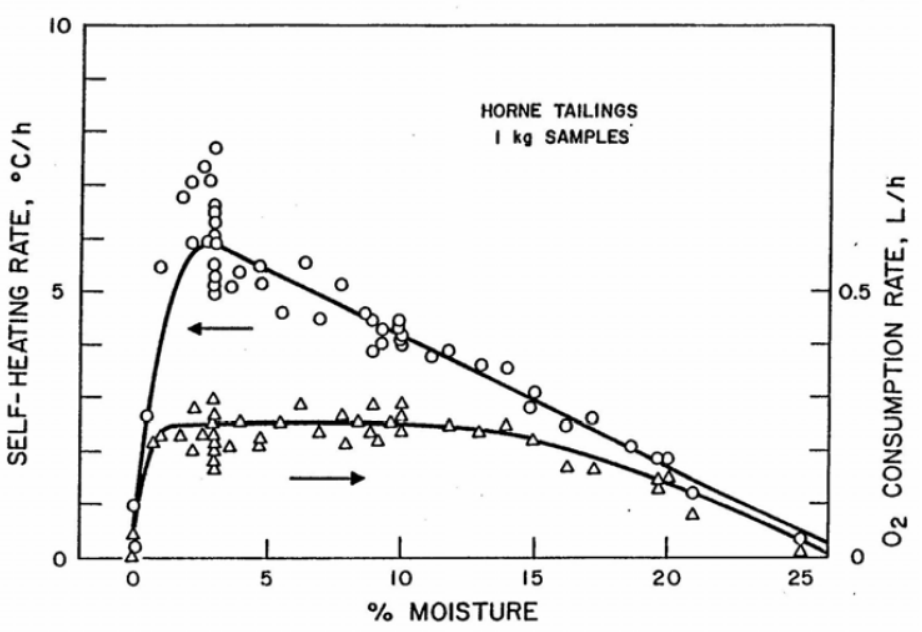

Figure 2.15 Moisture vs SHC. Reproduced with permission from (Rosenblum et al., 2001)

2.4.6 Particle Size

Numerous studies over the years have confirmed that in general, the oxidation rate is proportional to the surface area (Jiang *et al.*, 2000; Quanli *et al.*, 2007). As surface area increases in an equal mass of solid, more space is available for reactions to occur. Good (1997) determined that the ignition temperature decreases with decreasing particle size, and Rosenblum *et al.* (2001) showed that decreasing particle size increased the SHR. From Figure 2.16 below, it can be seen that in both stages of the FR experiment, the smaller particle size posed a greater SH threat than larger samples.

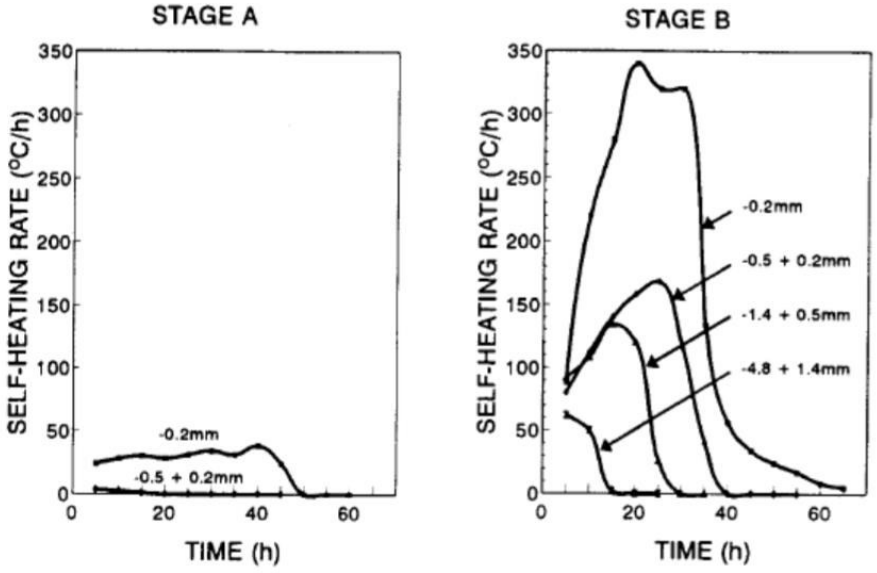

Figure 2.16 Particle size vs SHR. Reproduced with permission from (Rosenblum et al., 2001)

2.4.7 Galvanic Interaction

Most sulphide minerals are conductive, and their electrochemical behaviors can be characterized by their rest-potentials (Payant *et al.*, 2012; Rao & Finch, 1988). The rest-potentials of the rock-forming sulphides are listed in Table 2.2 below. Although these values vary depending on the origin of the mineral, the order generally remains consistent:

Pyrite > Chalcopyrite > Sphalerite > Pentlandite > Pyrrhotite > Galena

Table 2.2 Rest potential of sulphides. Adapted from (Payant et al., 2012)

Mineral	Formula	Rest Potential vs S.H.E
Pyrite	FeS_2	0.66 V
Chalcopyrite	$CuFeS_2$	0.56 V
Sphalerite	ZnS	0.46 V
Pentlandite	NiFeS	0.35 V
Pyrrhotite	Fe(1-x)S	0.31 V
Galena	PbS	0.28 V

Since sulphides in nature are commonly found as a part of a compound, when they are placed in an aqueous electrolyte, they become electrodes. The sulphide with the lower rest-potential acts as the anode and undergoes oxidation (electron giving), where as the sulphide with the higher rest-potential acts as the cathode (electron receiving). This electrochemical process is known as the "galvanic interaction", and the reactions are described in equations below.

Anodic (oxidation) half cell reaction:

$$MeS \rightarrow Me^{2+} + S^{o} + 2e^{-} \quad (2.4)$$

Cathodic (reduction) half cell reaction:

1) $1/2\ O_2 + H_2O + 2e^{-} \longrightarrow 2OH^{-}$ (2.5)

2) $Fe^{3+} + e^{-} \longrightarrow Fe^{2+}$ (2.6)

An example of galvanic interaction is shown in Figure 2.17. Assuming pyrite and chalcopyrite are undergoing galvanic reaction, pyrite becomes the anodic mineral and chalcopyrite becomes the cathodic mineral.

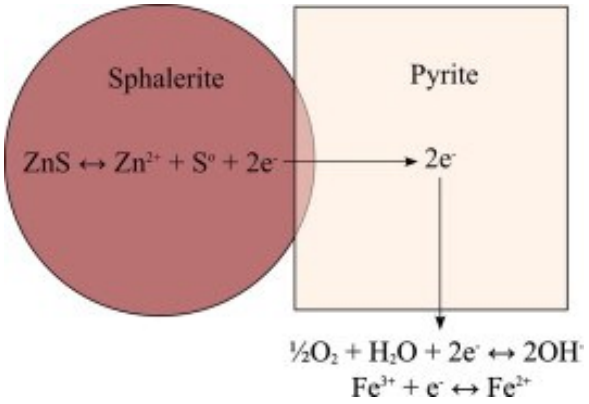

Figure 2.17 Galvanic interaction between pyrite and sphalerite. Reproduced with permission from (Payant et al., 2012)

Payant *et al.* (2012) showed that the presence of two minerals of sufficient difference in rest-potential (ΔE > 0.3) increases the chance of self-heating. They made binary sulphide mixture samples composed of different sulphides and subjected them to FR testing. The summary of sulphide mixtures and their difference in rest potentials are summarized in Table 2.3 below.

Table 2.3 Sulphide mixtures vs rest potential difference. Adapted from (Payant et al., 2012)

Mixtures	Rest potential difference (V)[3]
Pyrite - galena	0.45
Chalcopyrite – galena	0.35
Pyrite – chalcopyrite	0.1
Chalcopyrite - sphalerite	0.1

Figure 2.18 below shows that the mixtures with rest potential difference of greater then 0.3 exhibited high level of self-heating rate, compared to mixtures with low rest potential difference (ΔE ≤ 0.1).

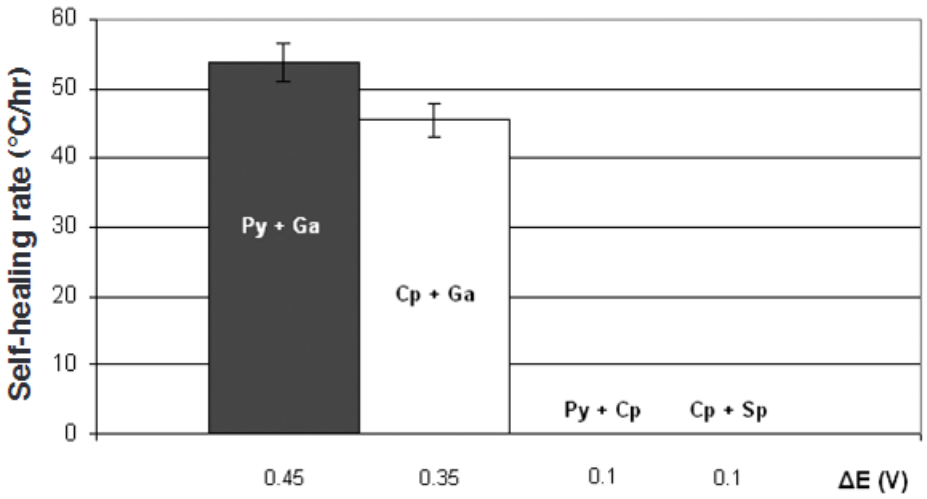

Figure 2.18 Self-heating rates for sulphide mixtures from standard test stage A. Reproduced with permission from (Payant & Finch, 2010)

2.4.8 Pyrrhotite Content

Pyrrhotite has a non-stoichiometric composition denoted as $Fe_{x-1}S_x$ where x is greater than 8 (Ex: Fe_7S_8, $Fe_{11}S_{12}$) (Belzile *et al.*, 2004). Therefore, it has an excess amount of sulphur that is free to react with oxygen. In comparison to pyrite (FeS_2), pyrrhotite has been shown to oxidize 20-100 times faster (Pearse, 1980). Belzile *et al.* (2004) theorized that when pyrrhotite is in an oxidizing environment, iron (Fe) diffuses outward to form an iron-oxyhydroxide layer at the air/solid interface, which promotes SH. Somot & Finch (2010) showed that sulphide minerals having pyrrhotite content of 10 wt.% or more have a higher propensity towards SH.

2.4.9 Temperature

The rule of thermodynamics states that as temperature increases, the rate of atomic diffusion also increases (Reed & Ehrlich, 1981). As more oxygen diffuses into the sulphide mineral, the formation of ferric oxides and elemental sulphur also increases (Steger, 1979).Rosenblum *et al.* (2001) demonstrated this positive correlation in the Figure 2.19 below, where the rate of sulphur

formation at higher temperatures (above 50°C) was exponentially higher than at lower temperatures (10°C).

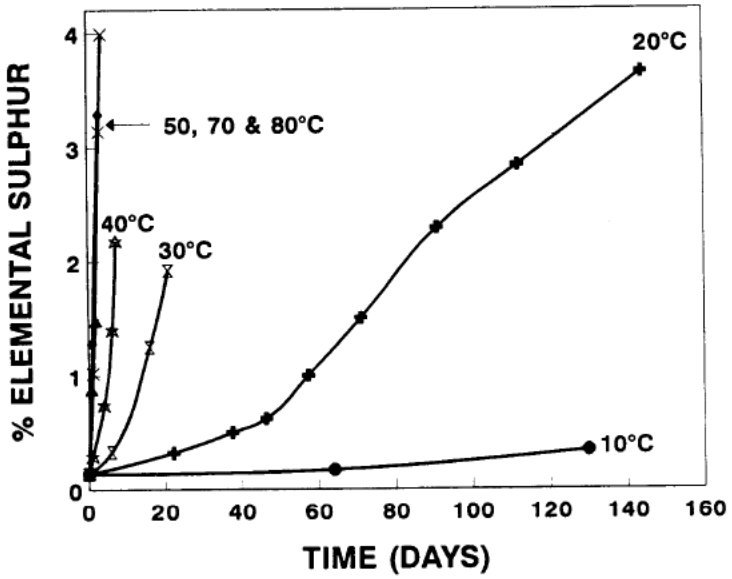

Figure 2.19 Temperature vs elemental sulphur formation. Reproduced with permission from (Rosenblum et al., 2001)

Rosenblum *et al.* (2001) also showed that the SHR increased with temperature in both Stage A and Stage B. From Figure 2.20 below, the test result showed that in Stage A, the self heating rate fell below the detection limit (1°C/h) at low temperatures, but rose above 35°C/h at 70°C, which is the standard testing temperature for Stage A. In Stage B, the test showed similar results, where the self heating rate fell below the detecting limit, which rose sharply to 120°C/h at 140°C (Rosenblum *et al.*, 2001).

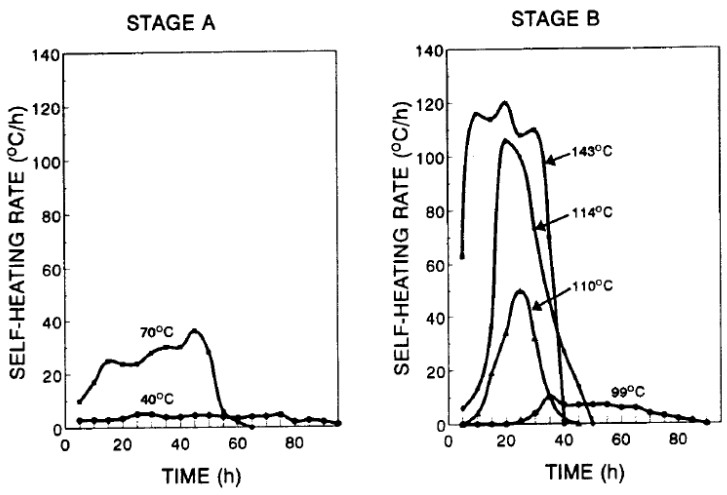

Figure 2.20 Temperature vs SHR in stage A and stage B. Reproduced with permission from (Rosenblum et al., 2001)

Numerous studies over the years have reported that the low temperature causes “delayed” SH reactions (Rosenblum & Spira, 1995) . Although this paper will continue the use of the term “delayed,” which was coined by Rosenblum & Spira (1995), other words have been used to describe this phenomenon. This “delayed” SH is highlighted in the Figure 2.21 below. Although the heating reactions are strong (peaks are well defined) for all temperatures once they initiate, at lower temperature (40°C) it took almost 50 hours for the reaction to begin.

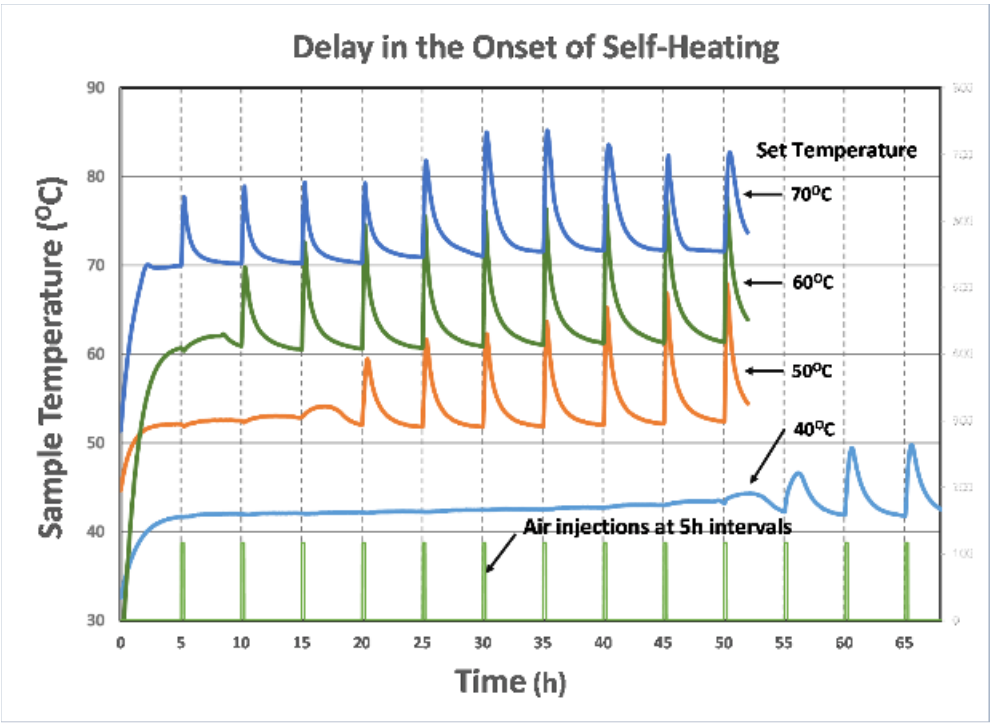

Figure 2.21"delayed" self heating. Reproduced with the permission from (Rosenblum et al., 2014)

2.4.10 Acidity

Previous studies have reported delay times ranging from minutes to many hours. Rosenblum *et al.* (2014) theorized that the delay at lower temperatures reflects the time required to acidify the water prior to H_2S generation. To test this theory, they weathered the samples with different water acidification levels and then subjected them to the FR test. The result shown in Figure 2.22 below demonstrates that using acidified water (pH: 0.43) rather than distilled water reduced the delay time to almost zero (Rosenblum *et al.*, 2014).

This finding is significant as it proves that the galvanic interaction (water acidification) phase precedes the subsequent thermodynamic heating phase *i.e*. once the oxide gangue is depleted, the heating reactions can begin (Belzile *et al.*, 2004; Rosenblum & Spira, 1995). In natural water environments at pH > 4, oxygen is the main oxidant of sulphide minerals; however, when the pH drops below 4, sulphides also begin to be oxidised by ferric iron (Rosenblum *et al.*, 2014). Since

ferric iron is a more reactive oxidising agent than oxygen under acidic conditions the SH reaction is quicker at lower pH.

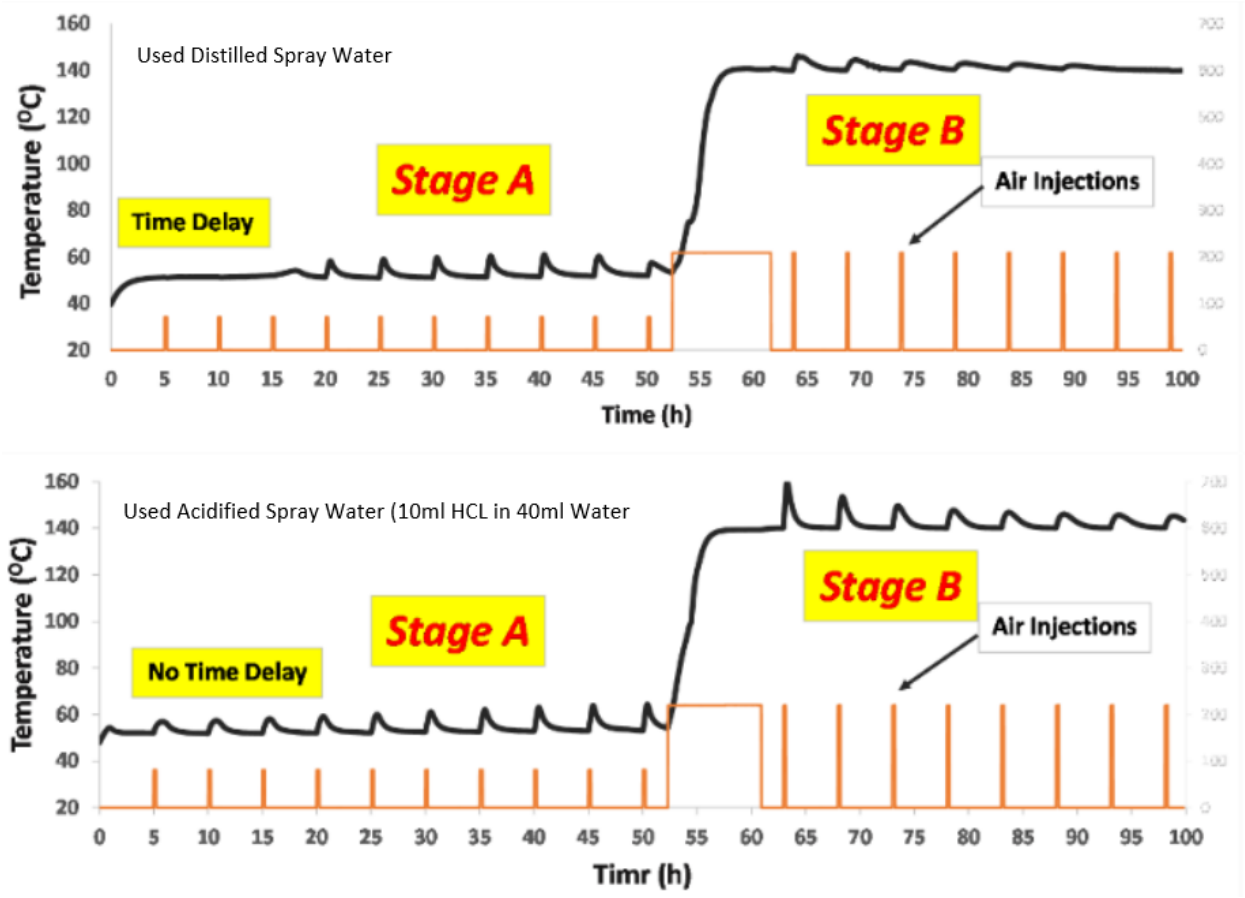

Figure 2.22 Acid and delay. Reproduced with permission from (Rosenblum et al., 2014)

2.5 Mechanism

The full extent of the sulphide mineral SH reactions is currently not fully understood. A wide range of chemical reactions are possible resulting in dissolved metals, sulphuric acid, sulphates, elemental sulphur etc. The following reactions are common SH reactions involving FeS_2 and Fe_7S_8 (Shaw *et al.*, 1998).

$$2\ FeS_2 + 7\ O_2 + 2\ H_2O \rightarrow 2FeSO_4 + 2\ H_2SO_4;\ \Delta H = -2558.4\ K\ J \quad (2.7)$$

$$4\ FeS2 + 15\ O2 + 14\ H2O \rightarrow 4\ Fe(OH)3 + 8\ H2SO4;\ \Delta H = -5092\ KJ \quad (2.8)$$

$$4\ FeS_2 + 15\ O_2 + 8\ H_2O \rightarrow 2\ Fe_2O_3 + H_2SO_4;\ \Delta H = -5740.5\ KJ \quad (2.9)$$

$$2\ Fe_7S_8 + 31\ O_2 + 2\ H_2O \rightarrow 14\ Fe_2SO_4 + 2H_2SO_4;\ \Delta H = -12590\ KJ \quad (2.10)$$

$$2\ FeS_2 + O_2 + 8\ H_2O \rightarrow Fe_2SO_4 \cdot H_2O + FeSO_4 \cdot 7H_2O;\ \Delta H = -1771.3KJ \quad (2.11)$$

$$12\ FeSO_4 + 3\ O_2 + 6\ H_2O \rightarrow 2\ Fe_2(SO_4)_3 + 4\ Fe(OH)_3\ \Delta H = -762\ KJ \quad (2.12)$$

$$4\ FeS + 3\ O_2 + 2\ H_2O \rightarrow FeO_4 \cdot OH + 4\ S^o \quad (2.13)$$

These equations can be simplified as (Shaw *et al.*, 1998):

$$Fe_{1-x}S + (2-x/2)O_2 + xH_2O \rightarrow (1-x)Fe^{2+} + SO^{2-}_4 + 2xH^+ \quad (2.14)$$

$$Fe^{2+} + 1/4O_2 + 5/2\ H_2O \rightarrow Fe(OH)_3 + 2H^+ \quad (2.15)$$

$$Fe_{1-x}S + (3-3x)O_2 + (12-12x)H^+ \rightarrow (4-4x)Fe^{3+} + 4S^o + (6-6x)H_2O \quad (2.16)$$

Under low oxygen conditions, ferrous sulphate ($FeSO_4$) and elemental sulphur (S^o) are principal products whereas in high oxygen conditions, ferric sulphate ($Fe_2(SO4)_3$) and Sulfuric acid H_2SO are formed as main products (Lukaszewski, 1973). In natural water environments, oxygen is the main oxidizer as can be seen by the above equations. However, Fe^{3+} becomes the main oxidizer in acidic environments.

The possible oxidation reactions involving Fe^{3+} are shown in the equations below.

$$Fe_{1-x}S + (8-2x)Fe^{3+} + 4H_2O \rightarrow (9+3x)Fe^{2+} + SO^{2-}_4 + 8H^+ \quad (2.17)$$

$$Fe_{1-x}S + (2-2x)Fe^{3+} \rightarrow (3-3x)Fe^{2+} + S^o \quad (2.18)$$

In Stage A, the sample increases in weight as the predominant reaction is the reaction of elemental sulphur (Rosenblum *et al.*, 2001). 80% to 96% of all oxidized sulphide create elemental sulphur.

There is an alternate theory of how elemental sulphur is generated. Somot & Finch (2010) discovered that when the acid (H^+) created in Equation (2.14) reacts with FeS, it generates H_2S.

This discovery was confirmed when the inserted copper pieces turned black in the presence of H_2S by forming Cu_2S after Stage A (Somot & Finch, 2010). With this discovery, they argued that there is an intermediary step between Stage A and the creation of elemental sulphur, which is shown by the following equation(Somot & Finch, 2010).

$$Fe_{1-x}S + 2H^+ \rightarrow (1-x)Fe^{2+} + H_2S \quad (2.19)$$

$$H_2S + 1/2O_2 \rightarrow 2/8S + H_2O \quad (2.20)$$

$$H_2S + O_2 \rightarrow SO + H_2O \quad (2.21)$$

$$H_2S + 3/2\ O_2 \rightarrow SO_2 + H_2O \quad (2.22)$$

$$H_2S + 2\ O_2 \rightarrow 2H_2SO_4 \quad (2.23)$$

$$2\ H_2S + S\ O_2 \rightarrow 3/8S + 2\ H_2O \quad (2.24)$$

Regardless of how the elemental sulphur is created, it is used in Stage B as a fuel, and oxidizes to produce heat (Moon *et al.*, 2019; Rosenblum & Spira, 1995).

$$S^o + O_2 \rightarrow SO_2 \quad (2.5)$$

2.6 Transition from Stage A to Stage B

There are two stable forms of elemental sulphur in nature, orthorhombic and monoclinic (Moon *et al.*, 2020). Moon *et al.* (2020) theorized that as SH progresses from Stage A to Stage B, the rhombic elemental sulphur that was formed in Stage A (alpha - S8) transforms into more reactive monoclinic sulphur (beta - S8).They highlighted that for this transition to occur, a favourable condition must be maintained, such as sufficient latent heat, and other factors forementioned in Section 2.4.

To visualize the latent heat, Moon *et al.* (2020) took 500g of active nickel concentrates, and performed an adiabatic FR test. An adiabatic test is where little to no heat flows in or out of the

sample. The results showed that the temperature remained roughly constant at around 96°C before continuing to rise. This shows that the transition occurs at 96°C, where the elemental sulphur transitioned from rhombic to monoclinic.

2.7 Mitigation

Various mitigation methods have been developed over the years to mitigate the potential hazards of sulphide SH (Farnsworth & Duties, 1977; Rosenblum *et al.*, 2017; Sipilä *et al.*, 2012). Since SH reactions are triggered by oxygen and moisture, most approaches focused on removing one (or more) of the reactants. These mitigation methods include: controlling pyrrhotite content to less than 10 wt.%; blanketing with CO_2 (in ships' holds and storage sheds); drying to less than 1 wt.% moisture; and shipping concentrates in bags (Sipilä *et al.*, 2012; Tributsch & Gerischer, 1976). Using chemical agents as suppressors grabbed the attention of many researchers in recent years. There are 2 main methods of chemical treatment, each highlighted by Rosenblum *et al*. (2017) and Jung *et al.* (2020). The impact of these chemicals on downstream processing such as flotation is still not fully understood and forms the basis of ongoing studies.

2.7.1 Coating Method

As mentioned in Section 2.5, H_2S is theorized to be the intermediate product that oxidizes to form elemental sulphur. Therefore, Rosenblum *et al.* (2017) theorized that if competing reactions with the H_2S are introduced, SH rates can be significantly reduced due to less elemental sulphur formation. To test this theory, they prepared a variety of lignosulfonate reagents and applied them to fresh nickel-sulphide ores before subjecting them to the FR test. The four lignosulfonates used in this experiment were D619 Sodium Lignosulfonate, D638 Calcium Lignosulfonate, D729 Ammonium Lignosulfonate and D748 Sodium Lignosulfonate. Using the copper lignosulfonate as

the example, the idea was that the Cu^{2+} would provide a competing reaction for H_2S to form copper sulphide (CuS), instead of undergoing SH reactions.

Figure 2.23 below shows the Stage A and B SHC values as a function of specified lignosulfonate concentrations (0, 2.5, 5, and 10 kg/t). All lignosulfonate types were successful at decreasing the SHC in both Stage A and B with as little as 2.5 kg/t. The test result also showed that SHC decreased with increasing lignosulfonate concentration, but only marginally (Rosenblum *et al.*, 2017).

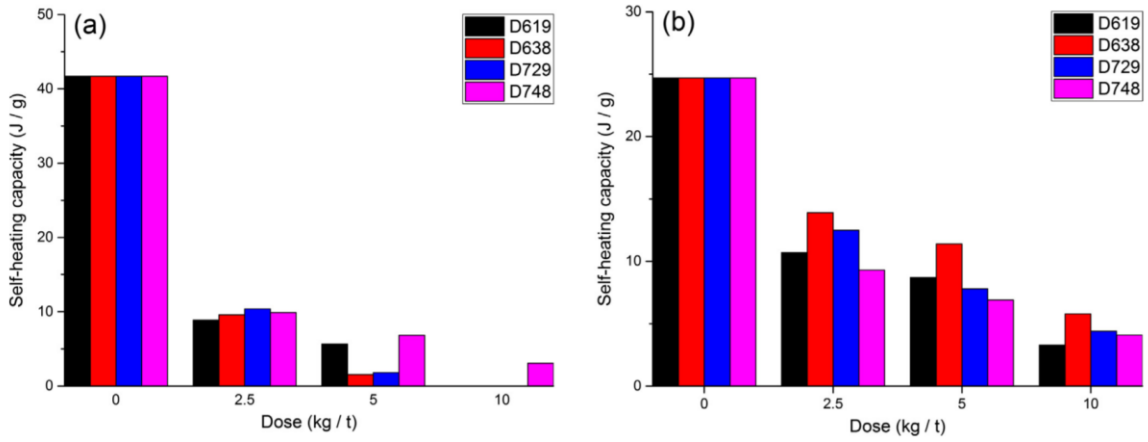

Figure 2.23 a) Coating method vs SHC Stage A and b) Coating method vs SHC Stage B. Reproduced with permission from (Rosenblum et al., 2017)

2.7.2 Moisture Removal Method

This method is more conventional in a sense that it focuses on removing one of the key ingredients of SH reactions. Jung *et al.* (2020) showed the potential use of hygroscopic reagents as a possible mitigation option. The five hygroscopic reagents that were used in their experiments and their corresponding water retention capacity are provided in Table 2.4 below.

Table 2.4 Hygroscopic reagent and their water retention. Adapted from (Jung et al., 2020)

Reagent	Water Retention (g/H_2O/kg reagent)
Sodium hydroxide	160
Sodium chloride	720
Drierite	350
Silica Gel	940
Poly (acrylic acid sodium salt)	690

250g of active sample with heavy (75 wt.%) pyrrhotite content was mixed with up to 100g of hygroscopic reagents and then subjected to the FR test. Using the SH assessment chart, the result shown in Figure 2.24 below shows that the two most affective reagents were silica gel, and poly (acrylic acid sodium salt) particles. The Silica gel was able to lower the risk from Zone 5 to Zone 2 ("will not heat beyond 100 °C") with 100g, and the poly particles were successful at lowering the risk to Zone 1 even with 50 g ("Safe")(Jung *et al.*, 2020).

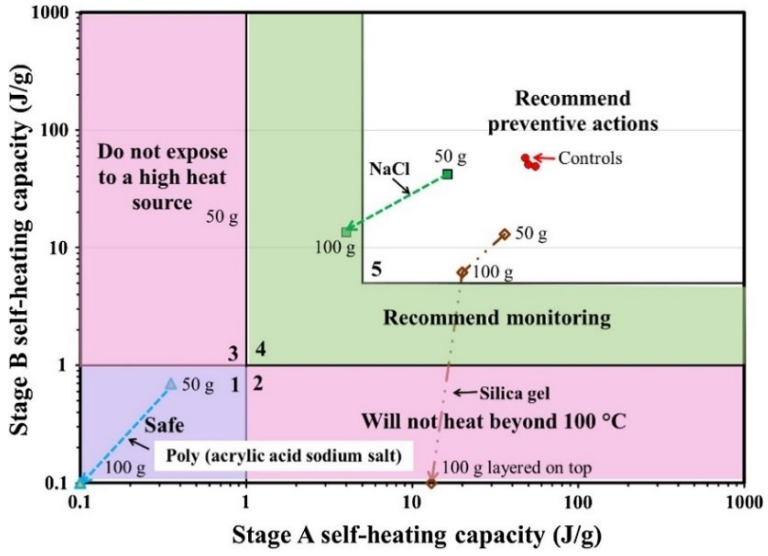

Figure 2.24 Hygroscopic reagent vs SHC. Reproduced with permission from (Jung et al., 2020)

Their success is attributed to their ability to hold water internally. Silica gel is made up of network of branched chains that creates a large specific surface area with exposed silanol groups (Si-OH).

The Silanol absorbs water by H-bonding, and the water is held internally by the linked chains preventing dissolution (Jung *et al.*, 2020; Ng *et al.*, 2001). Poly (acrylic acid sodium salt) particles consist of crosslinked coiled chains and it absorbs water by hydration and H-bonding (Buchholz & Peppas, 1994; Jung *et al.*, 2020). Similarly, the crosslinks allow swelling without particle dissolution.

Chapter 3 Role of Elemental Sulphur in Stage B Self-Heating of Sulphide Minerals, and the Potential Role of Polysulphides.

This chapter presents the scientific findings regarding the chemical interaction between elemental sulphur and sulphide minerals that fuel Stage B Self-Heating reactions. This analysis distinguishes conditioned sulphide minerals from unconditioned sulphide minerals. By conducting Stage B self-heating tests of elemental sulphur mixed with different materials, this paper found that only pyrrhotite could form a chemical interaction with elemental sulphur that could be found using XPS.

This chapter is a reproduction of the following published article:

Kim H, Rosenblum F, Kökkılıç O, Waters K. Role of Elemental Sulphur in Stage B Self-Heating of Sulphide Minerals, and the Potential Role of Polysulphides. *Minerals*. 2023; 13(7):923. https://doi.org/10.3390/min13070923

3.1 Abstract

Sulphide minerals undergo numerous stages of mineral processing to extract the desired metal. When they are exposed to certain environmental conditions, some sulphide minerals can spontaneously heat up, a process called self-heating (SH), which, if left unchecked, can be a major hazard. Self-heating occurs in three distinct temperature stages, termed Stage A (temperature below 100 °C), Stage B (temperature range of 100 °C – 350°C), and Stage C (above 350 °C). Historically, it was understood that elemental sulphur generated in Stage A fuels Stage B reactions; however, the full extent of this behaviour is still unknown. The aim of this study is to understand the role of elemental sulphur in Stage B reactions. The results have demonstrated that elemental sulphur is incapable of fueling Stage B self-heating on its own, and it needs to interact with sulphide minerals in ambient temperatures in the presence of moisture and air. This interaction seems to be unique to pyrrhotite, as it failed to demonstrate stage B self-heating with other sulphide minerals. Previous works in surface chemistry suggest that this interaction leads to the formation of polysulphides.

Keywords: self-heating; elemental sulphur; rock-forming sulphides

3.2 Introduction

Millions of tons of sulphide minerals are mined, processed, and stockpiled annually, as they are the source of numerous industrial metals, such as copper, nickel, lead, and zinc (Vaughan & Lennie, 1991). When they are exposed to the environment, especially moisture, sulphides have shown a propensity to oxidize and generate heat without an external heat source (i.e., self-heating) (Rosenblum et al., 2001). The detrimental effects of self-heating range from a minor impact on flotation to major disruptions, including the loss of equipment and fatalities (Good, 1977; Jung et al., 2020). Since the hazards were first documented by Good (1977), relatively minimal work has been published on the sulphide self-heating of ores and concentrates, with the exception of (Bertani et al., 2016; Dai, 2016; Navarra et al., 2010; Ngabe & Finch, 2014, 2014, 2014; Pan et al., 2015; Payant et al., 2012; Rosenblum et al., 2001; Rosenblum & Spira, 1981; Somot & Finch, 2010). The majority of the research on self-heating has been on the coal (Arisoy & Beamish, 2015; Nádudvari, 2014; Ribeiro et al., 2016) and wood industries (Cruz Ceballos et al., 2015).

Among the Rock-Forming sulphides (pyrite, pyrrhotite, chalcopyrite, sphalerite, and galena), pyrrhotite has exhibited the highest self-heating potential on its own (Payant et al., 2012). However, a variety of sulphide mineral mixtures with sufficient differences in their electrochemical potentials can undergo self-heating as well (Payant et al., 2012).

Self-heating occurs in three distinct stages, termed Stage A, Stage B, and Stage C. The role of elemental sulphur during different stages of self-heating reactions has been studied in the past (Rosenblum & Spira, 1995). It has been theorized that elemental sulphur generated during Stage A (from an ambient temperature to 100 °C) fuels Stage B self-heating reactions (from 100 °C

to 350 °C) (Rosenblum & Spira, 1995). This theory was further solidified when it was shown that the sulphur content increased from practically 0 wt.% to over 3 wt.% during Stage A (50 h at 70 °C) and decreased from 3 wt.% to 0 wt.% in Stage B (50 h at 140 °C) (Rosenblum & Spira, 1995). However, the mechanism of how elemental sulphur promotes Stage B self-heating is still not yet fully understood. The aim of this study is to investigate whether the addition of elemental sulphur will induce self-heating in Stage B for pure minerals and pyrrhotite-containing ore.

3.3 Materials and Methods

3.3.1 Samples

Samples of a massive sulphide ore mostly composed of magnetic pyrrhotite were taken from a mine in Northern Quebec, Canada. The samples were dried at the mine and shipped in airtight conditions. The purities of the sulphide minerals and the elemental sulphur used in this experiment pyrrhotite ore were verified via X-ray diffraction (XRD) (Bruker D8 Discover, Billerica, Massachusetts, USA). Figure 3.1 below shows that except for the received ore that contained quartz and pentlandite as minor impurities, the other minerals were of a high grade. The patterns were analyzed using DIFFRAC.EVA software (Bruker, Billerica, Massachusetts, USA), and reference data were collected from the International Centre for Diffraction Data (ICDD, 2022)

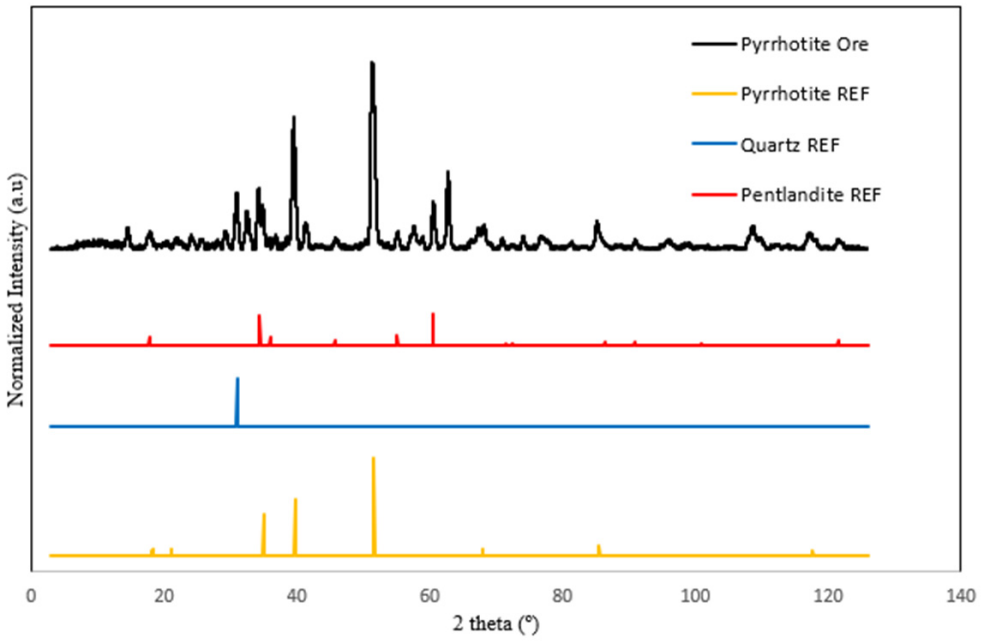
Pyrrhotite Ore
Pyrrhotite REF
Quartz REF
Pentlandite REF
Normalized Intensity (a.u)
0
20
40
60
80
100
120
140
2 theta (°)

(a)

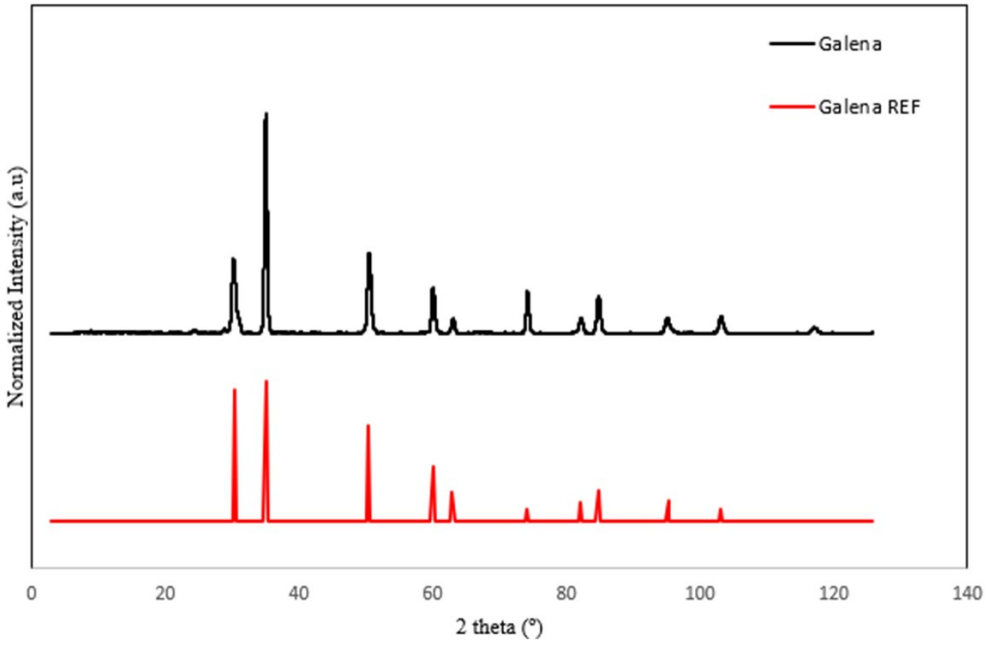
Galena
Galena REF
Normalized Intensity (a.u)
0
20
40
60
80
100
120
140
2 theta (°)

(b)

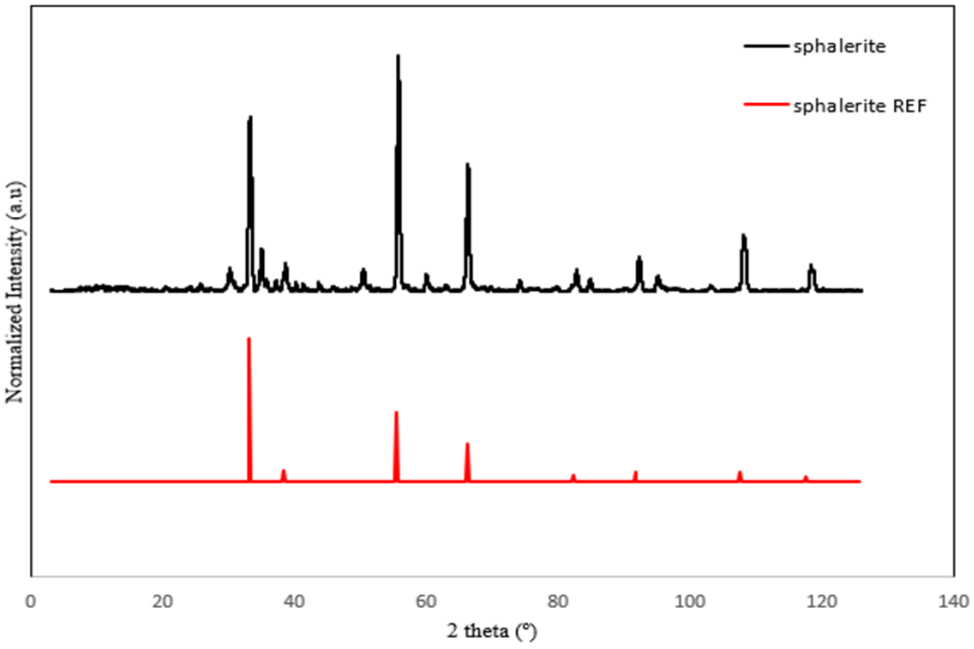
sphalerite
sphalerite REF
Normalized Intensity (a.u)
0
20
40
60
80
100
120
140
2 theta (°)

(c)

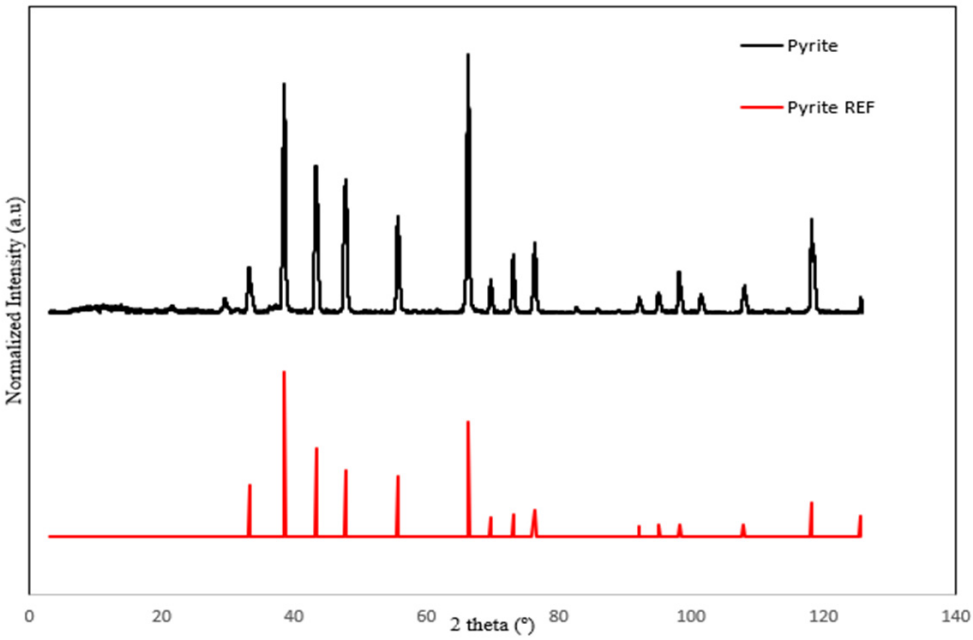
Pyrite
Pyrite REF
Normalized Intensity (a.u)
0
20
40
60
80
100
120
140
2 theta (°)

(d)

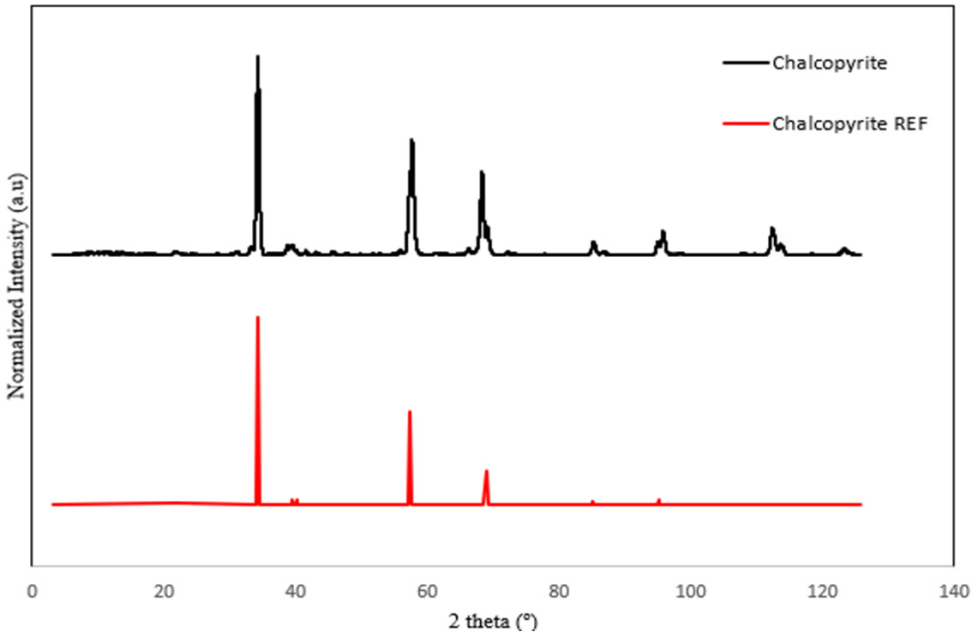

(e)

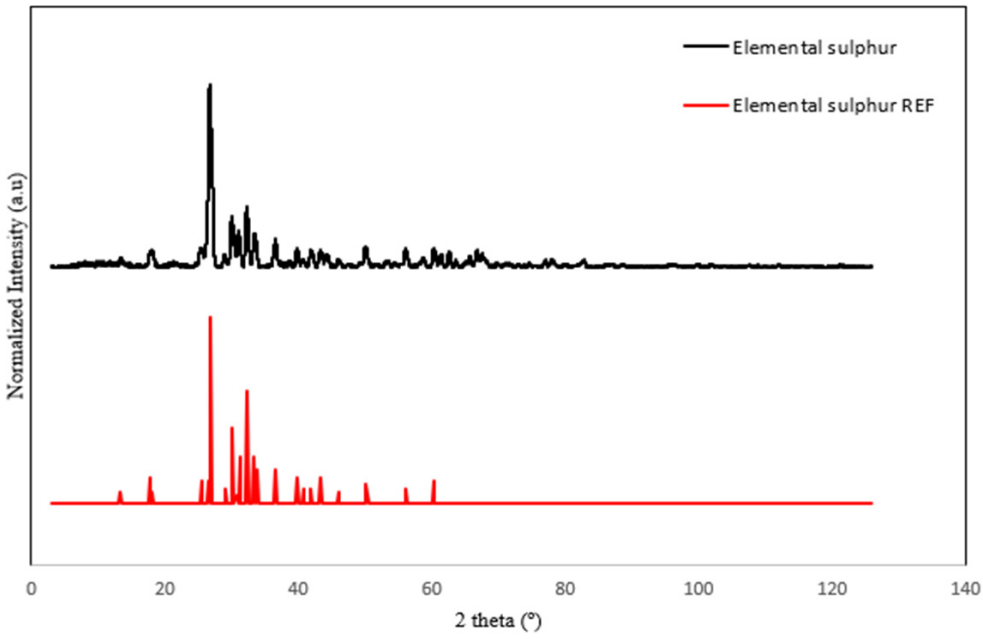

(f)

Figure 3.1. XRD patterns of (a) pyrrhotite ore, pyrite REF (PDF 00-042-1340), pyrrhotite REF (PDF 04-021-2764), and quartz REF (PDF 00-046-1045), (b) galena and galena REF (PDF 04-004-4329), (c) sphalerite and sphalerite REF (PDF 01-071-5976), (d) pyrite and pyrite REF (PDF 00-042-1340), (e) chalcopyrite and chalcopyrite REF (PDF 00-037-0471), elemental sulphur, and (f) elemental sulphur REF (PDF 00-008-0248).

Once received, the samples were finely ground using the Siebtechnik pulveriser type T100. The resulting material was split with a rotary splitter (Dickie & Stockler, Johannesburg, South Africa), and each portion weighed approximately 250 g. The ground samples were then kept at room temperature in sealed plastic bags. Other Rock-Forming mineral samples (pyrite, sphalerite, chalcopyrite, and galena) were purchased from Wards Science Plus (Rochester, New York, USA) and pulverized in the same manner as the pyrrhotite ore samples were. The 80% passing size (X80) of the sulphide minerals used in this research are shown in Table 3.1 below.

Table 3.1 Particle Size distribution

Sample	X_{80} (μm)
Pyrrhotite ore	150
Pyrite	233
Galena	240
Sphalerite	323
Chalcopyrite	203

Elemental sulphur powder was purchased from Alfa Aesar (Haverhill, MA, USA), with a 100% passing size (X100) of 44 μm. Elemental sulphur powder was kept at room temperature in its original packaging.

Silica sand powder (SiO2) was purchased from Sigma-Aldrich (St. Louis, MO, USA), with a 100% passing size (X100) of 44 μm. Silica sand powder was kept at room temperature in its original packaging.

3.3.2 FR Self-Heating testing apparatus

All tests for this study were conducted using the FR-2 self-heating apparatus. The apparatus consists of 5 major components, a 2L Pyrex Vessel, a constant-temperature coiled heater, a metal

mesh screen, a concrete base, and an insulator. The schematic of this apparatus is shown in Figure 3.2 below, adapted from (Rosenblum et al., 2001).

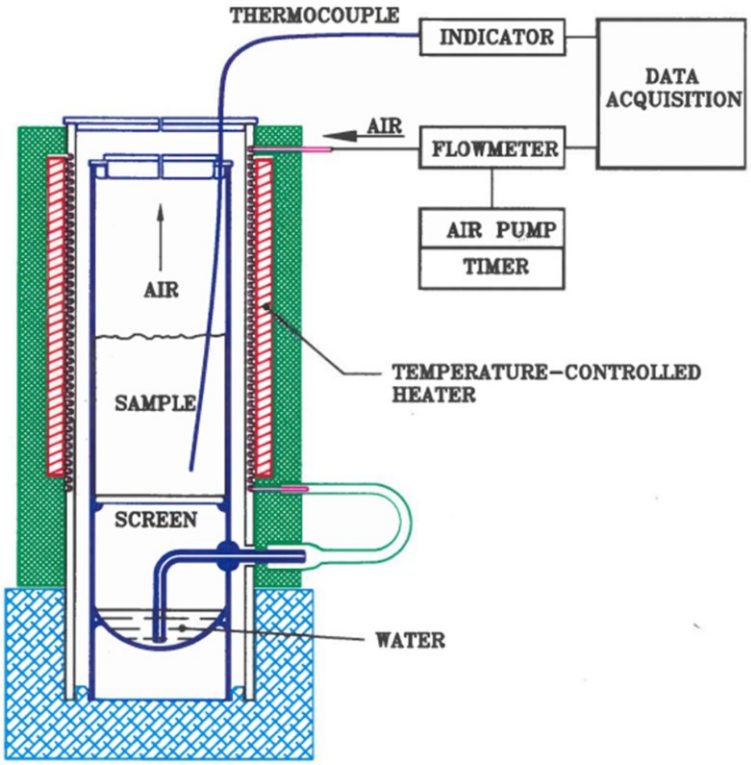

Figure 3.2 FR test apparatus.

Once the sample was placed in the 2L Pyrex Vessel, the temperature was raised in nitrogen (140 °C for Stage B) for each test. Once the equilibrium temperature was reached, 100 mL/min of air was injected for 15 min every 5 h for a total of 10 cycles (Rosenblum et al., 2001). The thermocouple was connected to a data logger to graph the temperature change over time, which recorded the sample temperature every minute. A reactive sample demonstrates a temperature increase with air injections, whereas a non-reactive sample shows the equilibrium temperature throughout the cycles.

For reactive samples, the Self-Heating Capacities (SHC) of the reactive samples were calculated using the following equation (Equation 3.1).

$$SHC_{\,i} = \sum SHR\left(\frac{^{\circ}C}{hr}\right)_{\,i} * Cp\left(\frac{J}{g*^{\circ}C}\right) * 0.25hr \quad (3.1)$$

Where: *SHC = Self Heating Capacity*
SHR = Self Heating Rate
Cp = Specific Heat Capacity
T = Time

The slopes of the temperature peak coincide with the Self Heating Rate (SHR) at the time of each of the 10 air injections. A single value of 0.6 J/g°C was used as specific heat capacity for all sulphide SHC calculations as it was found that nearly all the sulphides relevant to this work fell into the range from 0.5 J/g°C to 0.7 J/g°C over the relevant temperature range (from 25°C to 500°C) (Rosenblum et al., 2001). As the oxygen exposure time was capped at 15 minutes, the time (T) value was substituted with 0.25.

Therefore, Equation 3.1 was rewritten as:

$$SHC_{\,i} = \sum SHR_{\,i} * 0.6\left(\frac{J}{g^{\circ}C}\right) * 0.25hr \quad (3.2)$$

Simplified to:

$$SHC_{\,i} = \sum SHR_{\,i} * 0.15 \quad (3.3)$$

3.3.3 Surface Chemistry analysis – XPS

The elemental sulphur–sulphide chemical interface was analyzed via X-ray Photoelectron Spectroscopy (XPS) (Thermo Fisher Scientific, Waltham, MA, USA, Model K-Alpha). Experiments were carried out under the conditions of 50 eV pass energy, 200 µm X-ray size, and a chamber pressure of 10^{-7} Pa. Data collection and analysis were conducted using Avantage software (Thermo Fisher Scientific, Waltham, MA, USA, version 5.9931).

3.3.4 Sample Preparation and experimental procedure.

To determine whether the mixture of elemental sulphur and silica sand (chemically inert) could exhibit Stage B self-heating, 15g of elemental sulphur was added to 250g of silica sand and then subjected to the Stage B FR test.

To address whether pyrrhotite ore simply in contact with elemental sulphur could exhibit Stage B self-heating, a 250g pyrrhotite ore sample was mixed with 6 wt.% elemental sulphur and then subjected to the Stage B FR test.

For the context of this study, the term conditioning refers to a phase where moistened sulphide samples are mixed with elemental sulphur, and then exposed to the ambient environment for a given time while continuously blowing air. To address whether conditioned pyrrhotite ore could exhibit Stage B self-heating, 250 g of pyrrhotite ore sample and 6 wt.% elemental sulphur were mixed with 5 wt.% moisture and rested for 8 hr at 80 °C with a constant supply of air (100 mL/min). The conditioned sample was then subjected to the Stage B test.

Lastly, 250g of pyrite, galena, sphalerite, and chalcopyrite samples were mixed with 6 wt.% elemental sulphur and conditioned the same way before being subjected to the Stage B FR test.

3.4 Results and Discussion

3.4.1 Stage B Thermographs

3.4.1.1 Elemental sulphur

The Stage B thermograph of a mixture of silica sand and elemental sulphur is shown in Figure 3.3 below. The sample showed very little reactivity with each of the 10 air injections, and the total Self-Heating Capacity (SHC) of the sample remained at approximately 1.2 J/g. Based on this test result, it is evident that elemental sulphur alone does not pose the threat of Stage B self-heating.

This implies that elemental sulphur needs to interact with sulphide minerals to pose the threat of self-heating.

3.4.1.2 Unconditioned Mixture of Elemental Sulphur and Pyrrhotite Ore

A Stage B thermograph of the unconditioned mixture of pyrrhotite ore and elemental sulphur is shown in Figure 3.4 below. The sample again showed very little reactivity with air, and the total SHC was 2.5 J/g. Based on this test result, it can be observed that elemental sulphur simply in contact with pyrrhotite ore does not experience any Stage B self-heating. This result implies that for Stage B self-heating to occur, a previous step is needed in Stage A.

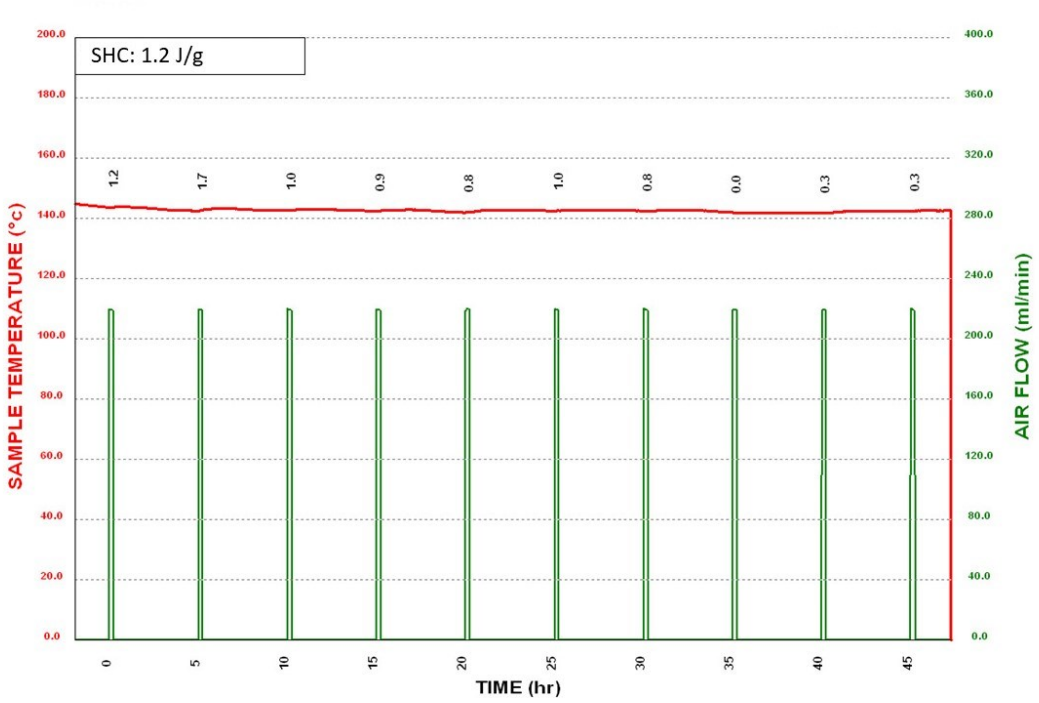

Figure 3.3 Thermograph of Elemental sulphur + silica sand

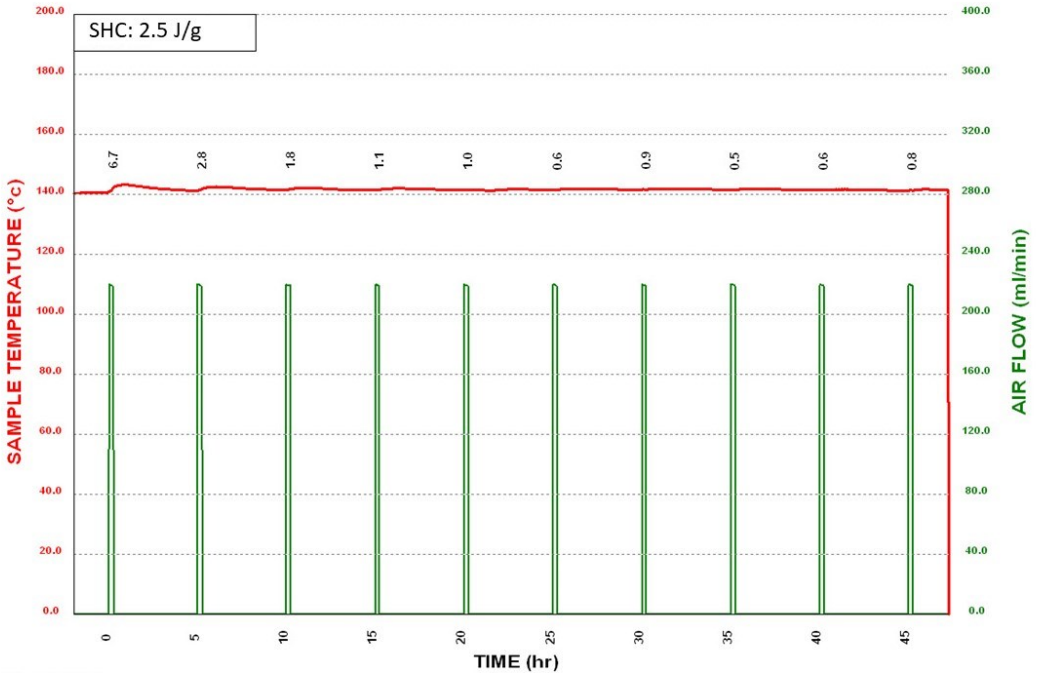

Figure 3.4 Thermograph of unconditioned pyrrhotite ore + elemental sulphur

3.4.1.3 Conditioned Mixture of Elemental Sulphur and Pyrrhotite Ore

A Stage B thermograph of the conditioned mixture of pyrrhotite ore and elemental sulphur is shown in Figure 3.5 below. The conditioned sample showed a very high propensity for Stage B self-heating. Based on this test result, it can be observed that elemental sulphur reacting with pyrrhotite ore in ambient conditions in the presence of air and moisture is a critical step, which then leads to Stage B self-heating.

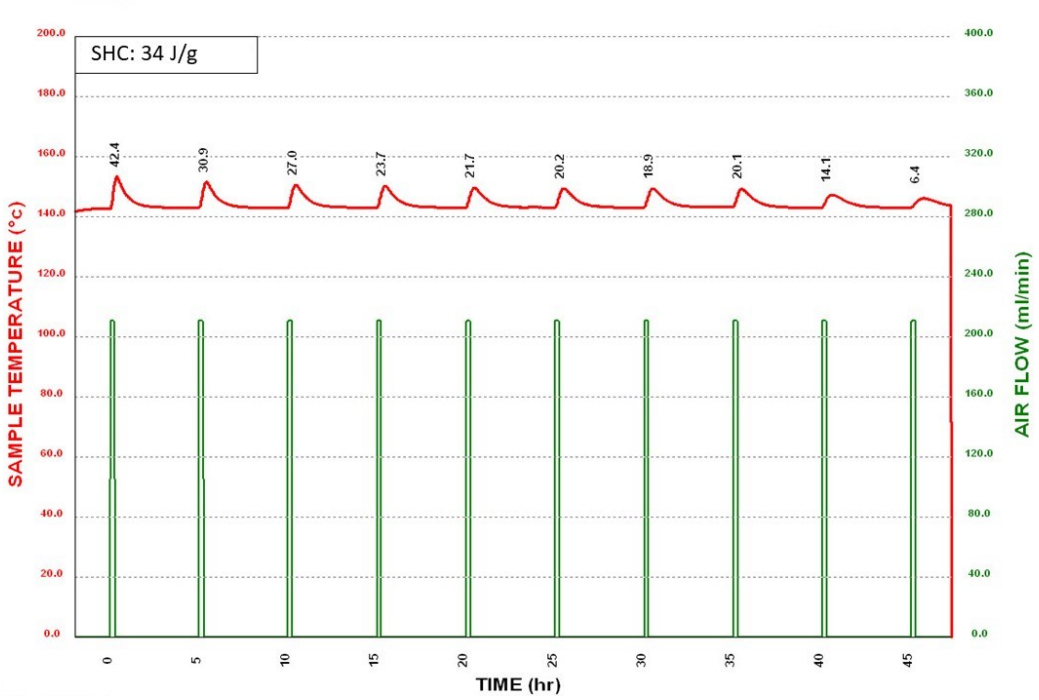

Figure 3.5 Thermograph of conditioned pyrrhotite ore + elemental sulphur

3.4.1.4 Generated elemental sulphur vs Added Elemental Sulphur

Since the conditioning phase is similar to Stage A, a distinction was drawn between the heat generated from artificially added elemental sulphur and the heat generated by elemental sulphur created during the conditioning phase. The result shows that although both samples demonstrated self-heating, the conditioned sample with added elemental sulphur had an SHC of 34 J/g (Figure 3.5), a value much higher than that of the sample without any sulphur added (Figure 3.6). It was highlighted in previous works that the self-heating rate in Stage B dropped to zero as the elemental sulphur content also dropped to zero (Rosenblum et al., 2001). This phenomenon can be observed in Figure 3.6, where after the first air injection, the peaks continuously decrease until becoming flat. This shows that the elemental sulphur that was generated during the conditioning phase depleted. However, when elemental sulphur was added

artificially and conditioned (Figure 3.5), the sample was highly reactive until the 8th air injection, before gradually diminishing.

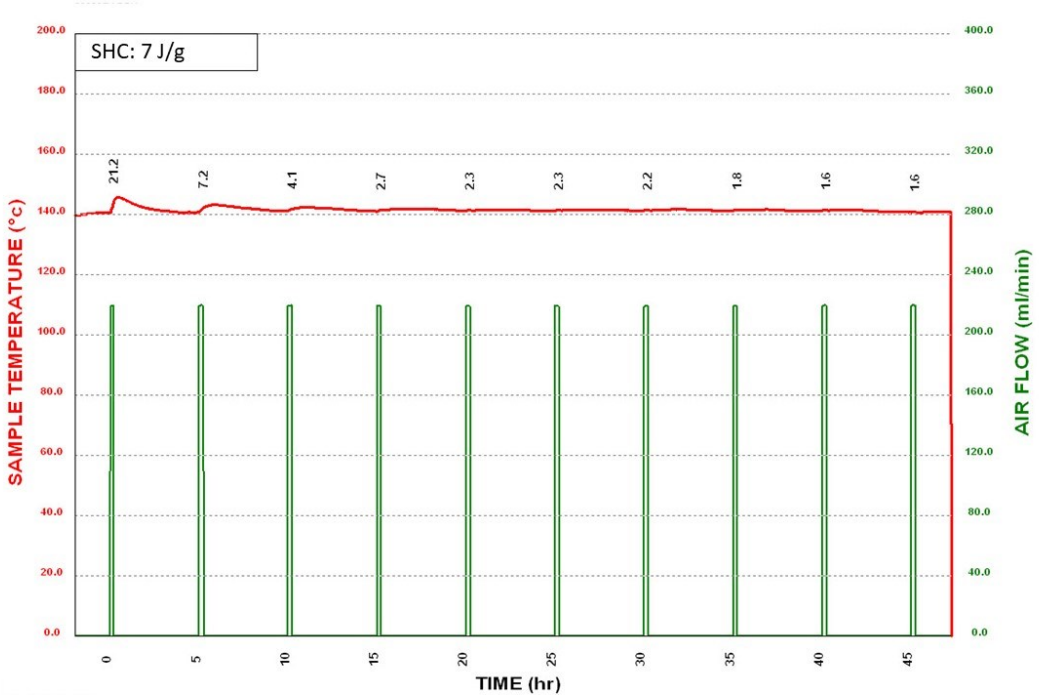

Figure 3.6 Thermograph of conditioned pyrrhotite ore

This shows that the source of the contribution of elemental sulphur to Stage B self -heating is irrelevant if it is given enough time to react with the pyrrhotite ore under Stage A conditions. This result strongly implies the formation of a chemical reaction between elemental sulphur and pyrrhotite ore in Stage A conditions.

3.4.1.5 Conditioned mixture of Elemental sulphur and other sulphide minerals

Thermographs of conditioned mixtures of pyrite, chalcopyrite, sphalerite, and galena with elemental sulphur are shown in Figure 3.7 below. None of the conditioned samples were reactive with incoming oxygen, showing SHCs of 3.7, 2.4, 0.2, and 2 J/g for pyrite, chalcopyrite, sphalerite, and galena, respectively. Based on these test results, it can be observed that with the exception

of pyrrhotite ore, conditioned mixtures of sulphide minerals and elemental sulphur do not experience Stage B self-heating.

3.4.2 XPS results

The change in chemical composition between the unconditioned and conditioned mixtures of elemental sulphur and pyrrhotite ore was investigated using XPS. The results are shown below in Figures 3.8 and 3.9. The unconditioned sample only has two distinct visible peaks, which correspond to elemental sulphur and pyrrhotite, respectively. However, the conditioned sample has three distinct peaks, which correspond to elemental sulphur, pyrrhotite, and polysulphide, respectively. The only notable difference is the presence of polysulphide, and it forms the basis of potential future studies. A summary of the peaks is shown in Table 3.2 below.

Table 3.2 Binding Energy

Mineral Compound	Binding energy	Reference
Pyrrhotite	163	(Lara et al., 2015)
Disulphide (S_2^{2-})	162	(Lara et al., 2015)
Elemental sulfur (S^o)	164.5	(Lara et al., 2015)
Polysulfides (S_n 2-)	164	(Lara et al., 2015)

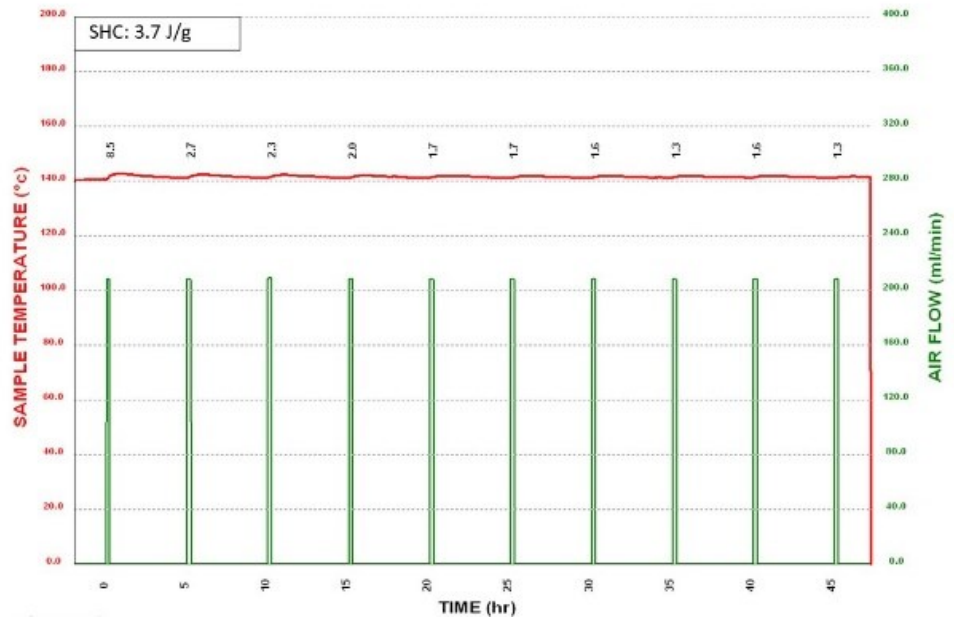
SHC: 3.7 J/g
SAMPLE TEMPERATURE (°c)
AIR FLOW (ml/min)
TIME (hr)

(a)

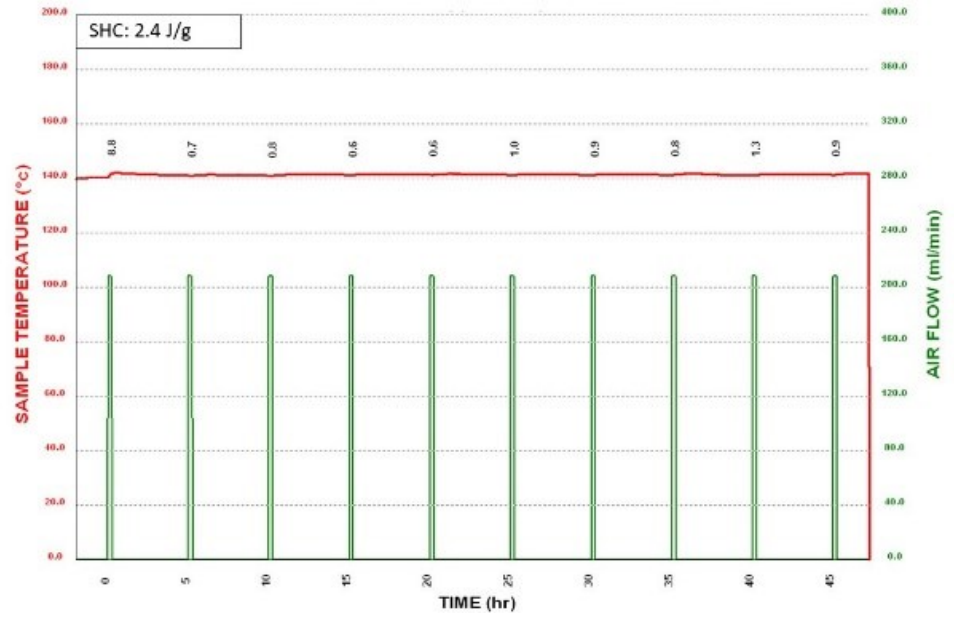
SHC: 2.4 J/g
SAMPLE TEMPERATURE (°c)
AIR FLOW (ml/min)
TIME (hr)

(b)

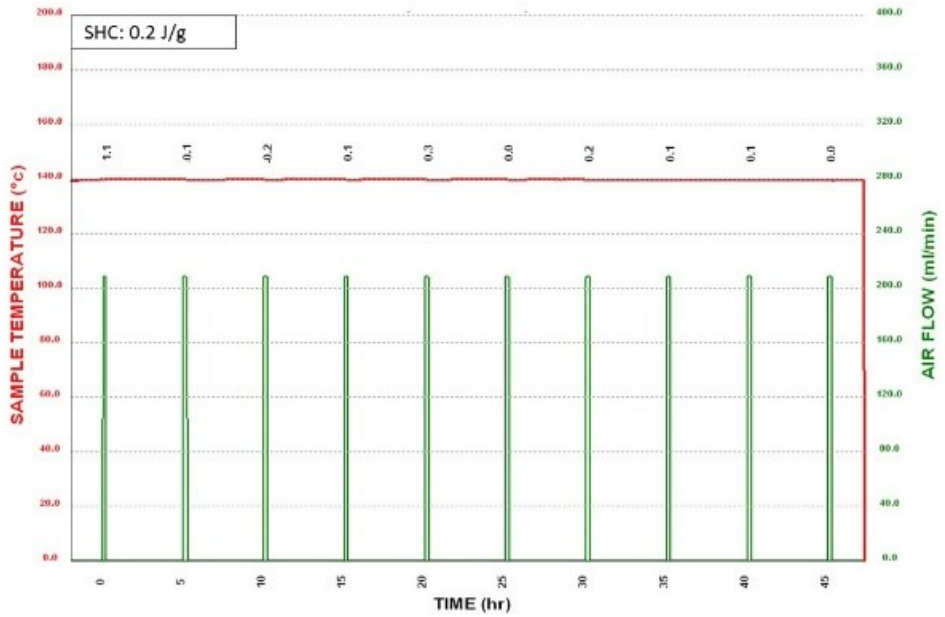

(c)

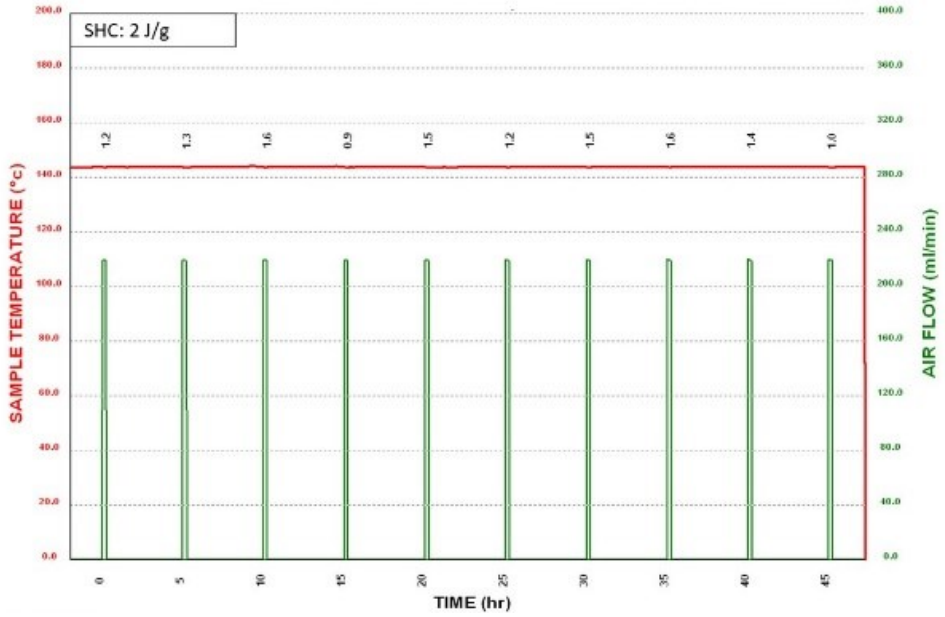

(d)

Figure 3.7 Thermographs of (a) conditioned pyrite + elemental sulphur (b) chalcopyrite + elemental sulphur (c) sphalerite + elemental sulphur (d) galena + elemental sulphur

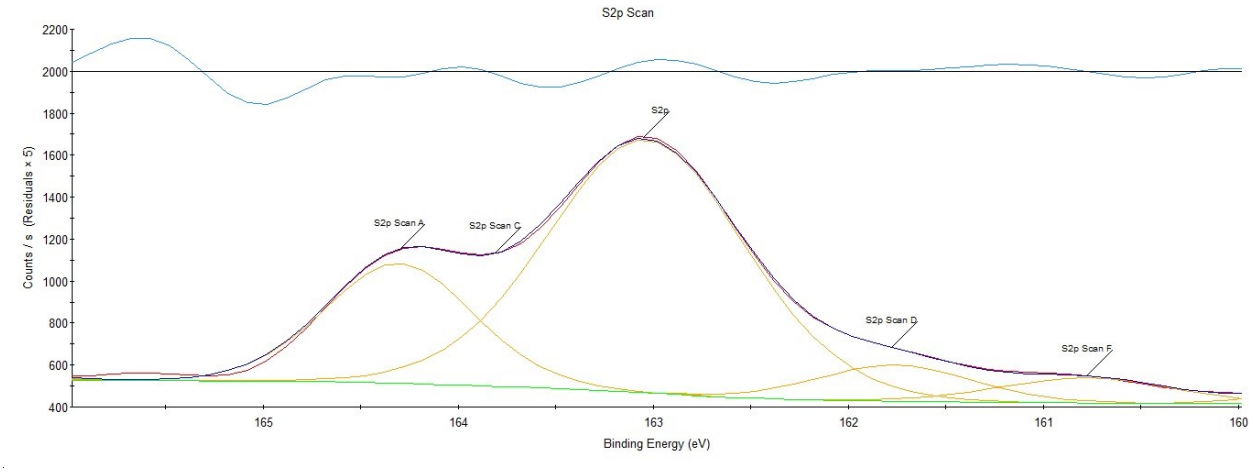

Figure 3.8 XPS of unconditioned mixture of pyrrhotite and elemental sulphur

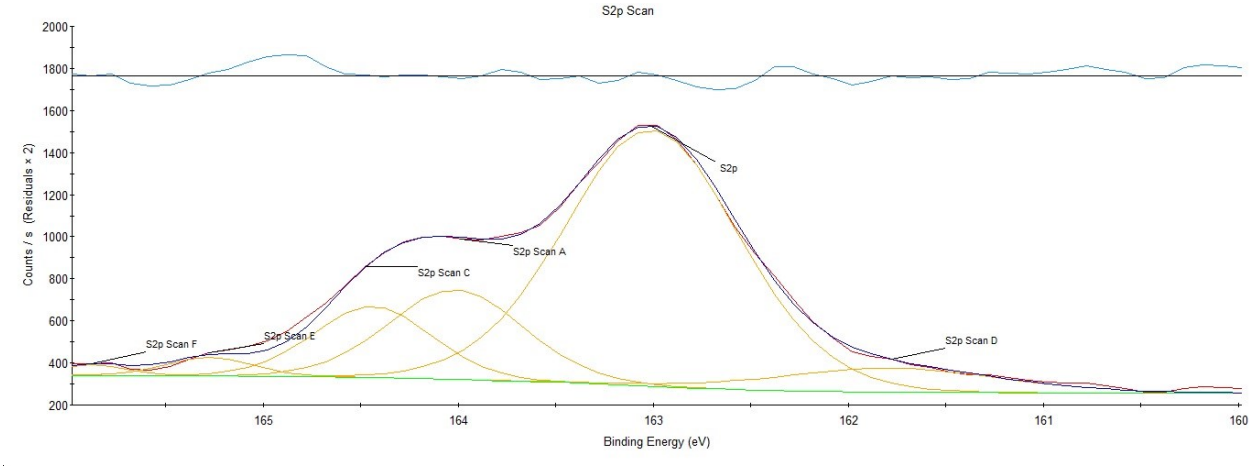

Figure 3.9 XPS of conditioned mixture of pyrrhotite and elemental sulphur

3.5 Conclusion

This study demonstrated that elemental sulphur on its own is incapable of influencing Stage B self-heating. Additionally, this study found that Stage B self-heating does not occur if elemental sulphur fails to form a necessary chemical connection with a sulphide mineral under ambient conditions. This chemical connection seems to be uniquely formed between pyrrhotite ore and elemental sulphur, as other Rock-Forming sulphide samples failed to demonstrate Stage B self-heating even after being conditioned.

Previous works on surface chemistry analysis suggest the possibility that Stage B self-heating is driven by polysulphides. However, more research is required.

Although this study showed that the elemental sulphur generated during the conditioning phase impacted the SHC minimally, future studies are required to clarify its impact on the overall reaction.

Author Contributions

Conceptualization, F.R., O.K. and K.W.; methodology, H.K. and F.R.; validation, F.R. and O.K.; formal analysis, H.K., F.R. and O.K.; investigation, H.K. and O.K.; Resources, K.W.; data curation, H.K.; writing—original draft, H.K.; writing—review and editing, F.R., O.K. and K.W.; supervision, K.W.; project administration, K.W.; funding acquisition, K.W. All authors have read and agreed to the published version of the manuscript.

Funding

The authors would like to acknowledge the Natural Science and Engineering Research Council of Canada (NSERC) in conjunction with SGS Canada Inc., COREM, Teck Resources Ltd., and Flottec Canada for funding this work through the Collaborative Research and Development Grant Program.

Conflict of interest

The authors declare no conflict of interest.

References

Arisoy, A., & Beamish, B. (2015). Mutual effects of pyrite and moisture on coal self-heating rates and reaction rate data for pyrite oxidation. Fuel, 139, 107-114.

Bertani, R., Biasin, A., Canu, P., Della Zassa, M., Refosco, D., Simionato, F., & Zerlottin, M. (2016). Self-heating of dried industrial tannery wastewater sludge induced by pyrophoric iron sulfides formation. Journal of Hazardous Materials, 305, 105-114.

Cruz Ceballos, D. C., Hawboldt, K., & Hellleur, R. (2015). Effect of production conditions on self-heating propensity of torrefied sawmill residues. Fuel, 160, 227-237.

Dai, Z. (2016). Development of an experimental methodology for sulphide self-heating studies and the self-heating tendency of Vale's Voisey's Bay Concentrator products. Minerals Engineering, 92, 125-133.

Good, B. (1977). The oxidation of sulphide minerals in the Sullivan mine. CIM Bulletin, 70(782), 83-88.

Jung, S., Tan, Y. H., Rosenblum, F., & Finch, J. A. (2020). Mitigating sulphide self-heating using hygroscopic agents: Case study with pyrrhotite. Minerals Engineering, 148, 106184.

Lara, R. H., Monroy, M. G., Mallet, M., Dossot, M., González, M. A., & Cruz, R. (2015). An experimental study of iron sulfides weathering under simulated calcareous soil conditions. Environmental Earth Sciences, 73(4), 1849-1869.

Nádudvari, Á. (2014). Thermal mapping of self-heating zones on coal waste dumps in Upper Silesia (Poland) — A case study. International Journal of Coal Geology, 128–129, 47-54.

Navarra, A., Graham, J., Somot, S., Ryan, D., & Finch, J. (2010). Mössbauer quantification of pyrrhotite in relation to self-heating. Minerals Engineering, 23(8), 652-658.

Ngabe, B., & Finch, J. A. (2014). Determination of specific heat capacity of sulphide materials at temperatures below 100° C in presence of moisture. Minerals Engineering, 58, 73-79.

Ngabe, B., & Finch, J. A. (2014). Self-heating activation energy and specific heat capacity of sulphide mixtures at low temperature. Minerals Engineering, 55, 154-161.

Ngabe, B., & Finch, J. A. (2014). Self-heating: Estimation of the heat release coefficient QA for Ni- and Cu-concentrates and sulphide mixtures. Minerals Engineering, 64, 126-130.

Pan, W., Wu, C., Li, Z.-j., & Yang, Y.-p. (2015). Self-heating tendency evaluation of sulfide ores based on nonlinear multi-parameters fusion. Transactions of Nonferrous Metals Society of China, 25(2), 582-589.

Payant, R., Rosenblum, F., Nesset, J. E., & Finch, J. A. (2012). The self-heating of sulfides: Galvanic effects. Minerals Engineering, 26, 57-63.

Ribeiro, J., Suárez-Ruiz, I., Ward, C. R., & Flores, D. (2016). Petrography and mineralogy of self-burning coal wastes from anthracite mining in the El Bierzo Coalfield (NW Spain). International Journal of Coal Geology, 154–155, 92-106.

Rosenblum, F., Nesset, J., & Spira, P. (2001). Evaluation and control of self-heating in sulphide concentrates. CIM Bulletin, 94(1056), 92-99.

Rosenblum, F., & Spira, P. (1981). Self-heating of sulphides 13th Annual Meeting of the Canadian Mineral Processors, Ottawa (Canada).

Rosenblum, F., & Spira, P. (1995). Evaluation of hazard from self-heating of sulphide rock. International Journal of Rock Mechanics and Mining Sciences and Geomechanics Abstracts,

Somot, S., & Finch, J. A. (2010). Possible role of hydrogen sulphide gas in self-heating of pyrrhotite-rich materials. Minerals Engineering, 23(2), 104-110.

Vaughan, D. J., & Lennie, A. R. (1991). The iron sulphide minerals: their chemistry and role in nature. Science Progress (1933-), 371-388.

Chapter 4 Exploring the Connection Between Elemental Sulphur and Sulphide Minerals During Stage A Conditions – a Design of Experiments Investigation

The previous chapter discussed the interaction between elemental sulphur and sulphides and discovered that their chemical interaction during ambient oxidation conditions are critical steps of self-heating. This chapter further examines the chemical connection between elemental sulphur and pyrrhotite by exploring multiple factors that influence the strength of their interactions. There are many discovered factors that influence self-heating reactions, and this study uses a Design of Experiments to rank the importance among the factors and determine their interactions.

This chapter is a reproduction of the following published technical note:

Kim, H., et al. "Exploring the Connection Between Elemental Sulphur and Sulphide Minerals During Stage A Conditions–Design of Experiments."

4.1 Abstract

Under certain conditions, sulphide minerals are susceptible to a phenomenon called Self-Heating (SH), where a material heats up without an external heat source. Self-heating is an exothermic oxidation reaction that occurs in three distinct temperature Stages, namely Stage A (room temperature to 100 °C), Stage B (100 °C – 350 °C), and Stage C (above 350 °C). New studies have shown that sulphide self-heating reactions are heavily influenced by the interaction between elemental sulphur and pyrrhotite ore during Stage A conditions. The aim of this study was to employ a Design of Experiments (DOE) method to investigate how differing Stage A conditioning parameters influence the interaction between elemental sulphur and pyrrhotite ore, and their effect on Self-Heating Capacity (SHC). The 5 main factors used to explore the differing Stage A conditions were elemental sulphur content, conditioning time, oxygen content, moisture content, and temperature. The optimum conditioning parameters that led to the highest degree of Self-Heating were calculated to be: 8.5 hr, 95°C, 80 ml air/min, 10 wt.% moisture, and 3 wt.% elemental sulphur.

Key words: Self-Heating, Pyrrhotite, Design of experiments

4.2 Introduction

Sulphide deposits are sources of many industrial metals such as copper and nickel, and precious metals such as gold and silver (Vaughan & Lennie, 1991). During various stages of mineral processing, sulphide ores (especially those containing pyrrhotite) can exhibit a temperature rise due to internal exothermic oxidation reactions, phenomena often referred to as "self-heating" or "spontaneous heating" (Rosenblum & Spira, 1995). Although self-heating related tragedies are rare in comparison to those tragedies caused by coal self-heating, reported cases date back to as early as the 1920s at the Sullivan lead-zinc mine in Canada (Jung et al., 2020; Nádudvari, 2014).

Previous research has shown that self-heating of sulphides occurs in 3 sequential stages, termed Stage A (ambient temperature to 100°C), Stage B (100 °C to 350 °C) and Stage C (above 350°C) (Rosenblum *et al.*, 2001; Rosenblum & Spira, 1995). Rosenblum and Spira (1995) showed that elemental sulphur was generated in Stage A, and it fuelled the self heating in Stage B. The sulphide self-heating reactions are susceptible to numerous factors ranging from galvanic interactions, temperature, oxygen availability, sample moisture, and conditioning time (time that the sample was exposed to a given environment) (Payant *et al.*, 2012; Rosenblum *et al.*, 2015; Rosenblum & Spira, 1995). However, these previous studies were focused on measuring the effects of individual factors on self-heating in Stage A (where elemental sulphur is formed) followed by Stage B (where elemental sulphur were consumed). Therefore, a comprehensive study that ranks the importance among the factors, and a study that measures the interaction between independent factors is still missing. In addition, the experiments proceed directly to Stage B, elemental sulphur is therefore artificially added.

The aim of this study was to investigate how certain factors influence Stage B self heating reactions during various conditioning parameters. This is the first study where a statistical Design of Experiments (DOE) was employed to measure the importance and interaction of independent factors in sulphide self-heating.

4.3 Experimental methodology

4.3.1 Sample

Samples of high-purity sulphide ore containing magnetic pyrrhotite were provided by a mine in Northern Quebec (Canada). The samples were dried at the mine and shipped in airtight conditions. Once received, these samples were finely ground using a Siebtechnik pulveriser (type T100), to achieve the 80% passing size (X_{80}) of approximately 150 µm. The samples were then split into 250g using a rotary splitter (Dickie & Stockler, Johannesburg, South Africa). The ground samples were then kept at room temperature in sealed plastic bags.

Elemental sulphur powder was purchased from Alfa Aesar (Haverhill, Massachusetts, USA), with a 100% passing size of 44 µm. Elemental sulphur powder was kept at room temperature in its original packaging.

X-ray diffraction (XRD) patterns (Bruker D8 Discover, Billerica, Massachusetts, USA, Co Kα source, λ = 1.79 Å) validated the purity of the elemental sulphur powder and showed that the ore contained quartz and pentlandite as minor impurities. The patterns were analyzed by DIFFRAC.EVA software (Bruker, Billerica, Massachusetts, USA), and it is given in the Appendix Figure A1.

4.3.2 FR Self-Heating Test

The pyrrhotite ore samples were conditioned for varying amounts of conditioning time, temperature, air flow (ml/min), wt.% moisture and wt.% sulphur, and were subjected to the Stage B FR self-heating tests. All tests for this study were conducted in the FR self-heating apparatus, following the test procedure documented by Rosenblum et al.(2001) and explained further in (Kim et al., 2023). The schematic of this apparatus and its procedure are given in the Appendix Figure A2. For the purpose of this study, the term “conditioning” refers to moistened sulphide samples mixed with elemental sulphur and allowed to rest in ambient temperature, while air was continuously passed through it.

4.3.3 Design of Experiments

Design of Experiments (DOE) is a statistical method to study the relationship between multiple factors and responses (Montgomery, 2017). This study employed Central Composite Experimental Design (CCD), which is the most common statistical experimental design method for optimization. A five-factor 2-level study was used to investigate the relationship between the independent variables (conditioning time, temperature, air (ml/min), wt.% moisture and wt.% sulphur), their effect on Stage B SHC, and possible interactions between the independent variables. The coded values were calculated and are given in the Appendix Table A1.

Analysis of Variance (ANOVA) is a powerful tool for determining the regression coefficients and detecting the statistical significance of the factors. Using the 95% confidence interval, the regression model is deemed acceptable if the calculated *p*-value from the ANOVA table is lower than 0.05. Optimization was realized by using contour plots for different interactions of two independent variables. It should be noted that “optimum” conditions in this case correspond to

the “worst case” scenario, where the self-heating would be most significant. Validation tests were carried out using the parameters determined by the overlaid contour plots. All statistical analysis was conducted by using the Minitab® Statistical Software (Minitab® LLC, State College, Pennsylvania, USA, version 21.1.1).

4.4 Results and Discussion

The second order regression model in coded units are shown as the following:

$$SHC = - -41.7 + 6.90\,x_1 + 0.760\,x_2 + 0.024\,x_3 - 7.01\,x_4 + 6.61\,x_5 - 0.1660\,x_1^2 - 0.00663\,x_2^2 - 0.00433\,x_3^2 + 0.105\,x_4^2 - 0.395\,x_5^2 - 0.0215\,x_1x_2 - 0.0118\,x_1x_3 - 0.119\,x_1x_4 - 0.188\,x_1x_5 + 0.00308\,x_2x_3 + 0.0721\,x_2x_4 - 0.0202\,x_2x_5 + 0.0585\,x_3x_4 - 0.0132\,x_3x_5 + 0.050\,x_4x_5 \quad (1)$$

Where:

x_1 = Conditioning Time (hr)

x_2= Temp (ºC)

x_3 = Air (ml/min)

x_4= Moisture (wt.%)

x_5 = Sulphur (wt.%)

The resulting Stage B SHCs are shown in the Appendix Table A2.

The F-value of the model was calculated to be 2.68. which is greater than the F-value found in the F-statistics Table with P = 0.05 ($F_{0.05(20,11)}$ = 2.64). The *p*-value of the model was 0.048, a smaller value than 0.05. The model had an R^2 of 82.95%, which is assumed to be a good fit as it had an R^2 value of greater than 80% (Azizi *et al.*, 2012; Joglekar *et al.*, 1987; Saguy & Graf, 1990). The given simplified ANOVA table and the normal probability and residual plots in the Appendix Table A3 and Figure A3, respectively, validate the model predictions. With these calculations, it

can be concluded that the regression models are acceptable and are suitable for modelling the response behaviors.

With the model validated, Student's t-test was conducted to evaluate the effectiveness of individual factors and interactions. The summary of Student's t-test including the *p*-value and T-value of each experimental parameter are shown in the Appendix Table A4. With a 95% confidence level, the *p*-values indicate the significance of variables and interactions, and T-values indicate whether each significant variable has a positive or negative effect on the response. T-values also measure the degree of significance, where the greater the T-value magnitude, the more significant it is. Five factors had a significant influence the on response, as they had a *p*-value lower than 0.05. These factors were: linear moisture term, quadratic conditioning time term, quadratic temperature term, quadratic sulphur content term, and quadratic air content term, which had *p*-values of 0.005, 0.025, 0.04, 0.023, and 0.035 respectively. With the respective T-values of 3.55, -2.59, -2.33, -2.63, and -2.40, their influence on the response is visualized in the Appendix Figure A4.

Although they did not satisfy the 0.05 threshold, from a practical point of view it is worth noting two extra interactions. The Air - Moisture interaction and Temperature - Moisture interaction both had *p*-values of 0.059 and 0.075, and T values of 2.1 and 1.97 respectively. This signifies that increasing air and temperature had a positive effect of moisture on SHC.

With the exception of moisture, all the other terms were quadratic, and had a negative T value. This signifies that increasing these factors had a positive effect on the response, but past a certain point, the SHC decreased.

To visualize the effect of variables over the experimental range, contour plots of the fitted models were used. The contour plots show the relationship between two independent variables and responses while the other variables are at the centre (0) level. The contour plots are shown in Figure 4.1 below.

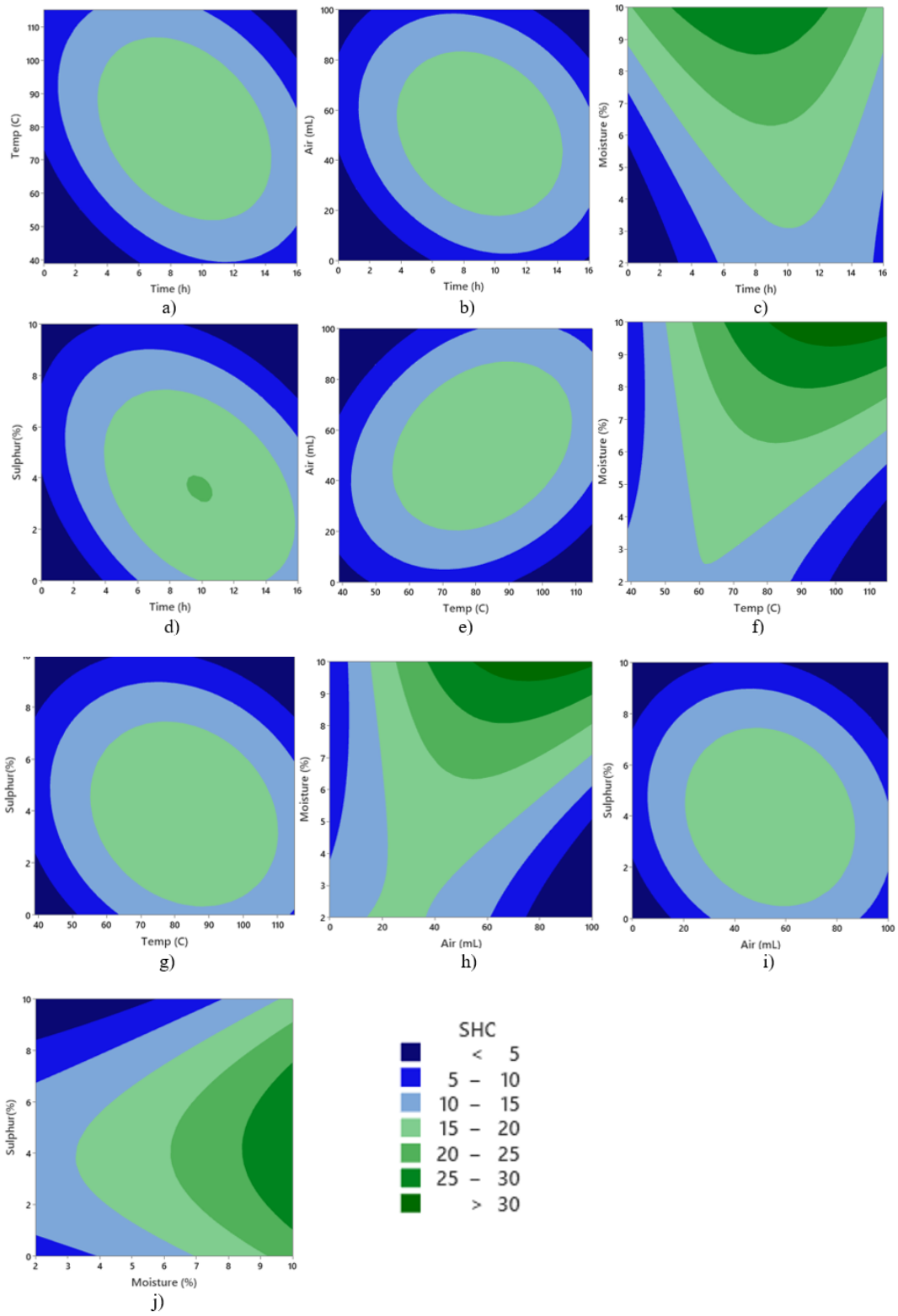

Figure 4.1 Contour plots of independent factors: a) Time and Temperature b) Time and Air c) Time and Moisture d) Time and Sulphur e) Temperature and air f) Temperature and Moisture g) Temperature and Sulphur h) Air and Moisture i) Air and Sulphur j) Moisture and Sulphur

As conditioning time increases (Figure 4.1 a – d), the chance for elemental sulphur to form a connection with the pyrrhotite ore increases. However, past a certain conditioning time, it may lead to a complete oxidation reaction. A completed oxidation reaction creates excess sulphates, which covers the surface and blocks the oxygen access (Rosenblum *et al.*, 2015).

As temperature increases (Figure 4.1 a, e, f, g), the thermodynamics are accelerated and may increase the connection between elemental sulphur and pyrrhotite ore. However, as temperature increases past a certain point moisture evaporates more rapidly (Rosenblum & Spira, 1995). Moisture is one of the two main components of self-heating reactions, an absence of which will result in no self-heating (Rosenblum *et al.*, 1982).

As sulphur content increases (Figure 4.1 d, g, i, j), SHC increases as more connections are formed between elemental sulphur and pyrrhotite ore. However, excess elemental sulphur could coat the surface, and block the oxygen access to elemental sulphur and pyrrhotite ore connection, like an oxide layer (Rosenblum *et al.*, 2015).

Oxygen is one of the fundamental factors of SHC as without it will cause no SHC. However as shown by Rosenblum *et al.* (2015), excess oxygen produces sulphate and impedes further oxidation reactions.

Although contour plots visualize the relationship between independent variables and their responses, they are limited in usage. This is because these plots use center levels (0) as references, therefore they cannot show the optimum range precisely if the optimum range does not lie in the center level. All optimum ranges for all independent variables were determined manually using contour plots and listed in the Appendix Table A5.

Overlaid contour plots can be used to optimize all responses simultaneously by emphasizing the overlaid region of the contour plots (Montgomery, 2017; Whitcomb & Anderson, 2004). The overlaid contours were plotted using the values from Appendix Table A5 and are shown in Figure 4.2 below. The black areas of the overlaid contours indicate the optimum conditioning parameters to get the highest Stage B SHC (> 30).

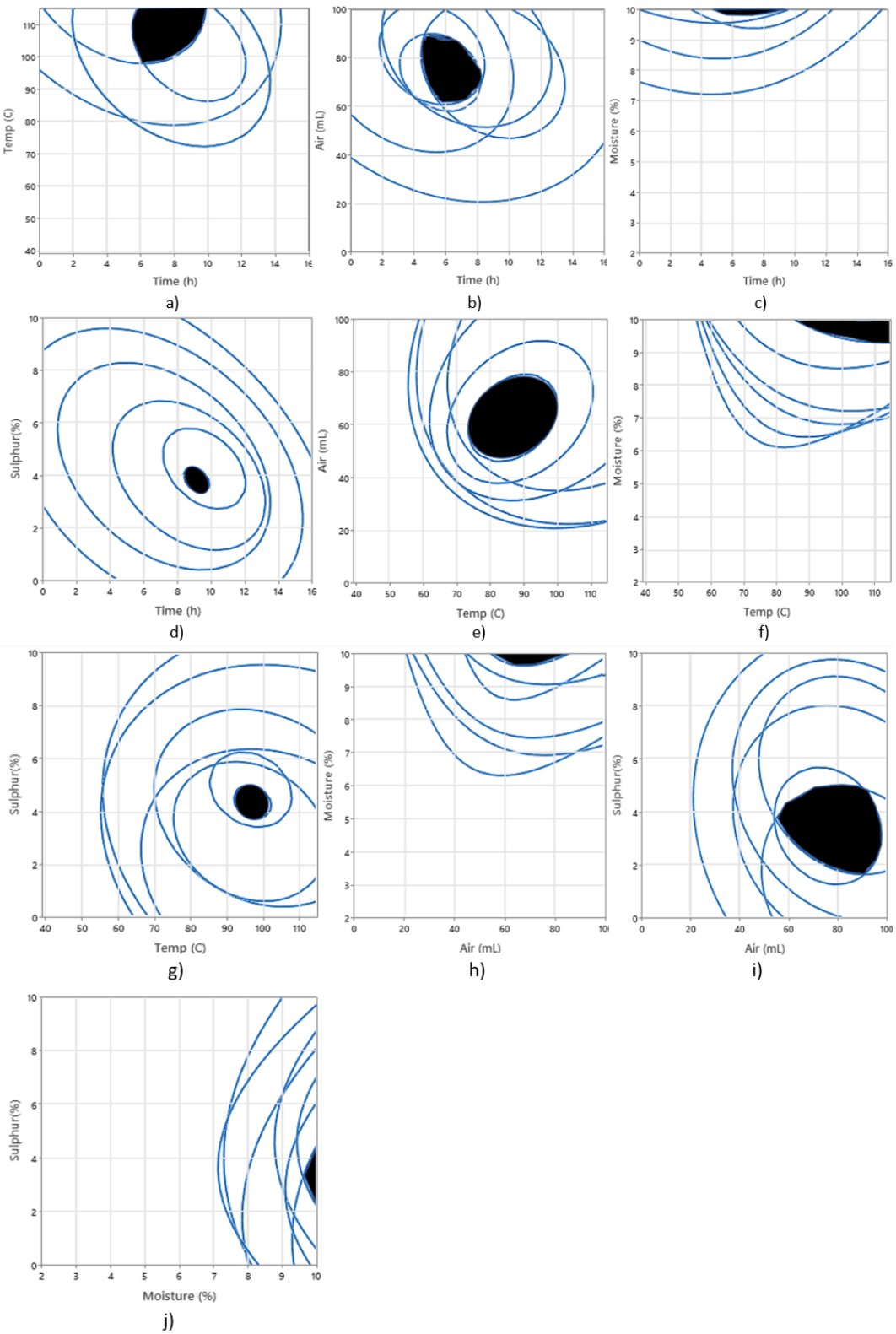

Figure 4.2 Overlaid contour plots a) Time and Temperature b) Time and Air c) Time and Moisture d) Time and Sulphur e) Temperature and air f) Temperature and Moisture g)Temperature and Sulphur h) Air and Moisture i) Air and Sulphur j) Moisture and Sulphur

Once the optimum range for each variable was estimated, validation tests were carried out to determine the final optimal points that could be present with high confidence and to confirm the validity of the models. It is important to note that the maximum temperature was capped at 95ºC, as the goal of this study was to understand the relationship between elemental sulphur and pyrrhotite during ambient conditioning phase (<100ºC). Above 96ºC, the transition from Stage A to Stage B begins to occur, and elemental sulphur transforms from rhombic elemental (alpha - S8) to monoclinic sulphur (beta - S8) (Moon *et al.*, 2020). The selected points, average of experimental results, fitted results from proposed models and errors are presented in the Appendix Table A6.

The highest SHC value of 42 (J/g) was obtained by using the following conditions: conditioning time 8.5 hr, temperature 95 ºC, Air (80 ml/min), Moisture (10 wt.%) and sulphur (3 wt.%). Exposing this pyrrhotite-rich ore to these conditions will lead to high degrees of Self-Heating, and this is to be avoided as high SHC has translated into tragedies in the past. (Jung *et al.*, 2020). The Stage B thermograph using these conditions are shown in the Appendix Figure A5.

It is important to note that SHC depends on a variety of factors such as particle size, acidity, and galvanic interaction, therefore the findings of this study might not directly correlate with the industry where the environmental conditions are uncontrolled.

4.5 Conclusion and Future Studies

A comprehensive study of factors that affect Stage B self-heating was conducted by using DOE. The 5-factor 2-level study showed that the most important factor was moisture content with a positive linear effect. Time, temperature, air content, and sulphur content had negative quadratic effects on SHC in Stage B. The optimum (i.e worst-case) conditioning parameters were calculated

to be: 8.5 hr, 95°C, 80 ml air/min, 10 wt.% moisture, and 3 wt.% elemental sulphur. Although the full explanation of why these factors affect SHC is not yet fully understood, the results are in line with past studies. (Rosenblum *et al.*, 2015; Rosenblum *et al.*, 2014). It is important to note that the SHC increased linearly as moisture content went up to 10 wt.%. However, from past literature, it is known that excess moisture content leads to SHC decrease, as it causes water-flooding (Rosenblum *et al.*, 2001). Therefore, increasing the moisture content to 12-15% or saturation would form part of an interesting future study.

Acknowledgements

The authors would like to acknowledge the Natural Science and Engineering Research Council of Canada (NSERC) in conjunction with SGS Canada Inc., COREM, Teck Resources Ltd., and Flottec Canada for funding this work through the Collaborative Research and Development Grant Program.

Contribution of authors

Conceptualization, Frank Rosenblum, Ozan Kökkılıç and Kristian Waters; methodology, Heekang Kim and Frank Rosenblum; validation, Frank Rosenblum and Ozan Kökkılıç; formal analysis, Heekang Kim, Frank Rosenblum and Ozan Kökkılıç; investigation, Heekang Kim and Ozan Kökkılıç; Resources, Kristian Waters; data curation, Heekang Kim; writing original draft, Heekang Kim; writing, review and editing, Frank Rosenblum, Ozan Kökkılıç and Kristian Waters; supervision, Kristian Waters; project administration, Kristian Waters; funding acquisition, Kristian Waters. All authors have read and agreed to the published version of the manuscript.

Conflict of Interest

The authors declare no conflict of interest.

References

Azizi, D., Shafaei, S. Z., Noaparast, M., & Abdollahi, H. (2012). Modeling and optimization of low-grade Mn bearing ore leaching using response surface methodology and central composite rotatable design. Transactions of Nonferrous Metals Society of China, 22(9), 2295-2305. https://doi.org/https://doi.org/10.1016/S1003-6326(11)61463-5

Joglekar, A. M., May, A. T., Graf, E., & Saguy, I. (1987). Product excellence through experimental design. Food product and development: From concept to the marketplace, 211.

Jung, S., Tan, Y. H., Rosenblum, F., & Finch, J. A. (2020). Mitigating sulphide self-heating using hygroscopic agents: Case study with pyrrhotite. Minerals Engineering, 148, 106184.

Montgomery, D. C. (2017). Design and analysis of experiments. John wiley & sons.

Moon, S., Rosenblum, F., Tan, Y., Waters, K. E., & Finch, J. A. (2020). Transition of sulphide self-heating from stage A to stage B. Minerals, 10(12), 1133.

Nádudvari, Á. (2014). Thermal mapping of self-heating zones on coal waste dumps in Upper Silesia (Poland)—A case study. International Journal of Coal Geology, 128, 47-54.

Payant, R., Rosenblum, F., Nesset, J., & Finch, J. (2012). The self-heating of sulfides: Galvanic effects. Minerals Engineering, 26, 57-63.

Rosenblum, F., Finch, J., Waters, K., & Nesset, J. (2015). A test apparatus for studying the effects of weathering on self-heating sulphides. Proceedings of the Conference of Metallurgists, Canadian Institute of Mining, Metallurgy and Petroleum, Toronto, ON, Canada,

Rosenblum, F., Nesset, J., & Spira, P. (2001). Evaluation and control of self-heating in sulphide concentrates. CIM Bulletin, 94(1056), 92-99.

Rosenblum, F., Nesset, J. E., Finch, J. A., & Waters, K. (2014). The key role of sample weathering in self-heating testing methodologies for sulphides. Review of self-heating testing methodologies. Proceedings of the XXVII International Mineral Processing Congress. Santiago.

Rosenblum, F., & Spira, P. (1995). Evaluation of hazard from self-heating of sulphide rock. International Journal of Rock Mechanics and Mining Sciences and Geomechanics Abstracts,

Saguy, I. S., & Graf, E. (1990). Food product development: from concept to the marketplace. Springer Science & Business Media.

Vaughan, D. J., & Lennie, A. R. (1991). The iron sulphide minerals: their chemistry and role in nature. Science Progress (1933-), 371-388.

Chapter 5 Comprehensive Scholarly Discussion

This thesis describes the new understandings of the self-heating mechanism. It was historically understood that self-heating of sulphides occurs in 3 distinct stages. It was understood that Stage A oxidation reaction creates elemental sulphur, and the Stage B oxidation reaction uses the elemental sulphur created during Stage A as fuel. However, this research found that as long as elemental sulphur forms the necessary connections with sulphide minerals during ambient oxidation reactions (Stage A), the source of elemental sulphur is irrelevant. To support the research findings in Chapter 3 and 4, Chapter 2 reviews the fundamental knowledge of sulphide self-heating. This chapter discusses the relationships among the chapters and their contributions to the overall objectives of this dissertation.

5.1 Comprehensive Discussion from Chapter 3

This chapter found that elemental sulphur created during Stage A does not pose a threat of self-heating on its own, and it needs to form a connection with sulphide minerals. This chapter also discovered that the source of elemental sulphur is irrelevant, and artificially added elemental sulphur can contribute to self-heating. After conducting self-heating tests of all rock-forming minerals (pyrrhotite, pyrite, galena, chalcopyrite, and sphalerite), It discovered that only pyrrhotite poses a threat of self-heating on its own. The XPS results revealed that the interaction between pyrrhotite and elemental sulphur during ambient oxidation reactions leads to the formation of polysulphides, which could potentially be the source of Stage B Self-Heating reactions. This knowledge could influence the safety protocols regarding safe storage of sulphide minerals.

5.2 Comprehensive Discussion from Chapter 4

There have been many studies in the past that revealed that self-heating is impacted by numerous factors. These factors include time, temperature, moisture content, oxygen content, and many more. However, this was the first study that included the artificially added elemental sulphur content as a factor. Additionally, this was the first study that took a statistical approach to rank the importance among the factors and determine the interaction among the factors. The DOE discovered 5 independent factors, and determined the optimum conditions that achieved the highest degree of Stage B SHC. The most optimum condition was found to be 8.5 hr, 95°C, 80 ml air/min, 10 wt.% moisture, and 3 wt.% elemental sulphur. These parameters could be used in future studies to bypass Stage A and reduce the self-heating testing times significantly. Also, these parameters could be used to improve single stage self-heating tests that doesn't account for weathering (U.N test). To elaborate, if the samples were conditioned using the parameters above and subjected to the U.N test, it would significantly reduce the risk of achieving false-negative tests.

Chapter 6 Conclusions, Contributions and Future studies

This research focused on exploring the deep connection between elemental sulphur and sulphide minerals. The objectives of this research were stated as:

1. To understand the chemical interaction between elemental sulphur and sulphide minerals during stage B conditions.
2. To evaluate the interactions between factors that influence the interaction between elemental sulphur and sulphide minerals.

The context and demand of these studies were presented, and research was conducted to fulfill these objectives. The results were presented as manuscript-based chapters (Chapter 3 and 4). The conclusions, future work and how the research contributed to the original knowledge are shown in the following sections.

6.1 Conclusions

Mechanisms of self-heating in different temperature zones.

- Elemental sulphur on its own, or simply in contact with sulphides does not promote self-heating.
- The link between elemental sulphur and pyrrhotite that is formed in Stage A conditions causes Stage B self-heating.
- The link between elemental sulphur and pyrrhotite is polysulphide.
- The link between elemental sulphur and pyrrhotite seems to be unique, as other “rock-forming” sulphides failed to replicate the data.

Interactions between factors that influence the self-heating reactions.

- The link between elemental sulphur and pyrrhotite is influenced by numerous factors such as time, temperature, moisture content, air content, and sulphur content.
- The 5-factor 2 level study showed that moisture had a linear proportional relationship, whereas the other factors had a negative parabolic relationship.
- The optimum conditioning parameters were determined to be: 8 hr, 85°C, 60 ml air/min, 10 wt.% moisture, and 3 wt.% elemental sulphur.

6.2 Future work

- Determine other factors that influence the relationship between elemental sulphur and pyrrhotite.
- Deeper surface chemistry analysis of the link between elemental sulphur and pyrrhotite
- Determine whether the different superstructures of pyrrhotite have different self-heating characteristics.

Master References

Azizi, D., Shafaei, S. Z., Noaparast, M., & Abdollahi, H. (2012). Modeling and optimization of low-grade Mn bearing ore leaching using response surface methodology and central composite rotatable design. Transactions of Nonferrous Metals Society of China, 22(9), 2295-2305. https://doi.org/https://doi.org/10.1016/S1003-6326(11)61463-5

Beever, P. F., & Crowhurst, D. (1989). Fire and explosion hazards associated with milk spray drying operations. International Journal of Dairy Technology, 42(3), 65-70.

Belzile, N., Chen, Y.-W., Cai, M.-F., & Li, Y. (2004). A review on pyrrhotite oxidation. Journal of geochemical exploration, 84(2), 65-76.

Buchholz, F. L., & Peppas, N. A. (1994). Superabsorbent polymers: science and technology. ACS Publications.

Carras, J. N., & Young, B. C. (1994). Self-heating of coal and related materials: models, application and test methods. Progress in Energy and Combustion Science, 20(1), 1-15.

Deer, W. A., Howie, R. A., & Zussman, J. (1978). Rock-forming Minerals: Feldspars, Volume 4A.

Farnsworth, D., & Duties, S. (1977). Introduction to and background of sulphide fires in pillar mining at the Sullivan Mine. CIM Bulletin, 70(782), 65-71.

Good, B. (1977). The oxidation of sulphide minerals in the Sullivan mine. CIM Bulletin, 70(782), 83-88.

Guidotti, T. (1996). Hydrogen sulphide. Occupational Medicine, 46(5), 367-371.

Jiang, W., Nadeau, G., Zaghib, K., & Kinoshita, K. (2000). Thermal analysis of the oxidation of natural graphite—effect of particle size. Thermochimica Acta, 351(1-2), 85-93.

Joglekar, A. M., May, A. T., Graf, E., & Saguy, I. (1987). Product excellence through experimental design. Food product and development: From concept to the marketplace, 211.

Jung, S., Tan, Y. H., Rosenblum, F., & Finch, J. A. (2020). Mitigating sulphide self-heating using hygroscopic agents: Case study with pyrrhotite. Minerals Engineering, 148, 106184.

Kim, H., Rosenblum, F., Kökkılıç, O., & Waters, K. (2023). Role of Elemental Sulphur in Stage B Self-Heating of Sulphide Minerals, and the Potential Role of Polysulphides. Minerals, 13(7), 923. https://www.mdpi.com/2075-163X/13/7/923

Legge, A., & Krupa, S. (2002). Effects of sulphur dioxide. Air pollution and plant life, 2, 135-162.

Lukaszewski, G. (1973). Sulphides in underground mine filling operations.

McCutcheon, S. R., & Walker, J. A. (2019). Great Mining Camps of Canada 7. The Bathurst Mining Camp, New Brunswick, Part 1: Geology and Exploration History. Geoscience Canada: Journal of the Geological Association of Canada/Geoscience Canada: journal de l'Association Géologique du Canada, 46(3), 137-154.

Montgomery, D. C. (2017). Design and analysis of experiments. John wiley & sons.

Moon, S., Rosenblum, F., Tan, Y., Waters, K. E., & Finch, J. A. (2020). Transition of sulphide self-heating from stage A to stage B. Minerals, 10(12), 1133.

Moon, S., Rosenblum, F., Tan, Y. H., Nesset, J. E., Waters, K. E., & Finch, J. A. (2019). Examination of the United Nations self-heating test for sulphides. Canadian Metallurgical Quarterly, 58(4), 438-444.

Nádudvari, Á. (2014). Thermal mapping of self-heating zones on coal waste dumps in Upper Silesia (Poland)—A case study. International Journal of Coal Geology, 128, 47-54.

Ng, K. C., Chua, H., Chung, C., Loke, C., Kashiwagi, T., Akisawa, A., & Saha, B. B. (2001). Experimental investigation of the silica gel–water adsorption isotherm characteristics. Applied Thermal Engineering, 21(16), 1631-1642.

Ngabe, B., & Finch, J. A. (2014). Self-heating activation energy and specific heat capacity of sulphide mixtures at low temperature. Minerals Engineering, 55, 154-161.

Payant, R., Rosenblum, F., Nesset, J., & Finch, J. (2012). The self-heating of sulfides: Galvanic effects. Minerals Engineering, 26, 57-63.

Payant, R., Rosenblum, F., Nesset, J. E., & Finch, J. A. (2012). The self-heating of sulfides: Galvanic effects. Minerals Engineering, 26, 57-63. https://doi.org/https://doi.org/10.1016/j.mineng.2011.10.019

Payant, R. A., & Finch, J. A. (2010). The Effect of Sulphide Mixtures on Self-Heating. Canadian Metallurgical Quarterly, 49(4), 429-434. https://doi.org/10.1179/cmq.2010.49.4.429

Pearse, M. (1980). Chemical study of oxidation of sulphide concentrates.

Quanli, J., Haijun, Z., Suping, L., & Xiaolin, J. (2007). Effect of particle size on oxidation of silicon carbide powders. Ceramics international, 33(2), 309-313.

Rao, S. R., & Finch, J. (1988). Galvanic interaction studies on sulphide minerals. Canadian Metallurgical Quarterly, 27(4), 253-259.

Reed, D. A., & Ehrlich, G. (1981). Surface diffusion, atomic jump rates and thermodynamics. Surface Science, 102(2-3), 588-609.

Reimers, G. W., & Hjelmstad, K. E. (1987). Analysis of the oxidation of chalcopyrite, chalcocite, galena, pyrrhotite, marcasite, and arsenopyrite (Vol. 9118). US Department of the Interior, Bureau of Mines.

Rosenblum, F., Finch, J., Waters, K., & Nesset, J. (2015). A test apparatus for studying the effects of weathering on self-heating sulphides. Proceedings of the Conference of Metallurgists, Canadian Institute of Mining, Metallurgy and Petroleum, Toronto, ON, Canada,

Rosenblum, F., Nesset, J., & Finch, J. (2014). Review of Self-Heating Testing Methodologies. 46th Annual Canadian Mineral Processors Operating Conference, Ottawa, Ontario,

Rosenblum, F., Nesset, J., Moon, S., Finch, J., & Waters, K. (2017). Reducing the self-heating of sulphides by chemical treatment with lignosulfonates. Minerals Engineering, 107, 78-80.

Rosenblum, F., Nesset, J., & Spira, P. (2001). Evaluation and control of self-heating in sulphide concentrates. CIM Bulletin, 94(1056), 92-99.

Rosenblum, F., Nesset, J. E., Finch, J. A., & Waters, K. (2014). The key role of sample weathering in self-heating testing methodologies for sulphides. Review of self-heating testing methodologies. Proceedings of the XXVII International Mineral Processing Congress. Santiago.

Rosenblum, F., & Spira, P. (1995). Evaluation of hazard from self-heating of sulphide rock. International Journal of Rock Mechanics and Mining Sciences and Geomechanics Abstracts,

Rosenblum, F., Spira, P., & Konigsmann, K. (1982). Evaluation of hazard from backfill oxidation. CIM bulletin,

Saguy, I. S., & Graf, E. (1990). Food product development: from concept to the marketplace. Springer Science & Business Media.

Shaw, S., Groat, L., Jambor, J., Blowes, D., Hanton-Fong, C., & Stuparyk, R. (1998). Mineralogical study of base metal tailings with various sulfide contents, oxidized in laboratory columns and field lysimeters. Environmental Geology, 33(2), 209-217.

Sipilä, J., Auerkari, P., Heikkilä, A.-M., Tuominen, R., Vela, I., Itkonen, J., Rinne, M., & Aaltonen, K. (2012). Risk and mitigation of self-heating and spontaneous combustion in underground coal storage. Journal of Loss Prevention in the Process Industries, 25(3), 617-622.

Somot, S., & Finch, J. (2006). High self-heating rate of pyrrhotite-rich material–H2S as a fuel. Proceedings of the 38th Annual Meeting of the Canadian Mineral Processors of CIM. Ottawa,

Somot, S., & Finch, J. A. (2010). Possible role of hydrogen sulphide gas in self-heating of pyrrhotite-rich materials. Minerals Engineering, 23(2), 104-110.

Steger, H. (1979). Oxidation of sulphide minerals—VI Ferrous and ferric iron in the water-soluble oxidation products of iron sulphide minerals. Talanta, 26(6), 455-460.

Tanackov, I., Janković, Z., Sremac, S., Miličić, M., Vasiljević, M., Mihaljev-Martinov, J., & Škiljaica, I. (2018). Risk distribution of dangerous goods in logistics subsystems. Journal of Loss Prevention in the Process Industries, 54, 373-383.

Tributsch, H., & Gerischer, H. (1976). The oxidation and self-heating of metal sulphides as an electrochemical corrosion phenomenon. Journal of Applied Chemistry and Biotechnology, 26(1), 747-761.

United.Nations. (2011). Classification procedures, test methods and criteria relating to class 2, class 3, class 4, division 5.1, class 8 and class 9. In Recommendations on the Transport of Dangerous Goods: Manual of Tests and Criteria - Fifth Revised Edition. United Nations. https://doi.org/doi:https://doi.org/10.18356/bbaae943-en

Vaughan, D. J., & Corkhill, C. L. (2017). Mineralogy of sulfides. Elements, 13(2), 81-87.

Vaughan, D. J., & Lennie, A. R. (1991). The iron sulphide minerals: their chemistry and role in nature. Science Progress (1933-), 371-388.

Whitcomb, P. J., & Anderson, M. J. (2004). RSM Simplified: Optimizing Processes Using Response Surface Methods for Design of Experiments (1st Edition ed.). Productivity press. https://doi.org/https://doi.org/10.4324/9780367806071

Yang, F., Wu, C., & Li, Z. (2011). Investigation of the propensity of sulfide concentrates to spontaneous combustion in storage. Journal of Loss Prevention in the Process Industries, 24(2), 131-137.

Yang, J., Li, X., & Liu, Q. (2017). China's copper demand forecasting based on system dynamics model.

Appendix

Additional data for Chapter 4 “Exploring the Connection Between Elemental Sulphur and Sulphide Minerals During Stage A Conditions – a Design of Experiments Investigation”

Sample characterization

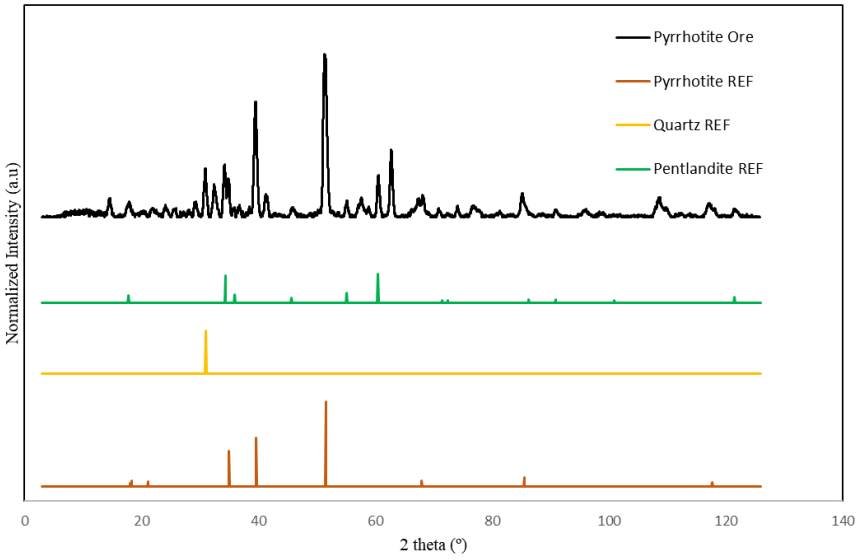

a)

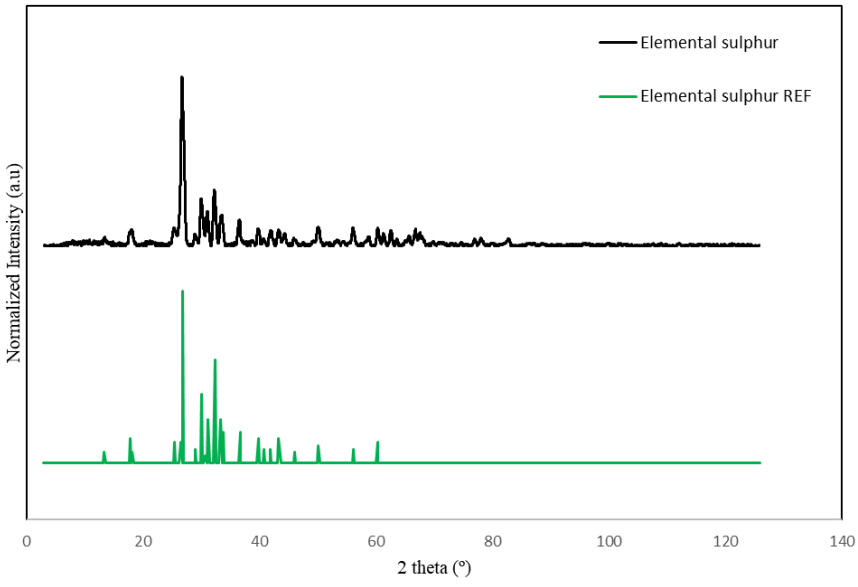

b)

Figure A1. XRD pattern of a) pyrrhotite-rich ore pyrite REF (PDF 00-042-1340), pyrrhotite REF (PDF 04-021-2764), and quartz REF (PDF 00-046-1045) b) elemental sulphur, and elemental sulphur REF (PDF 00-008-0248).

Test Procedure

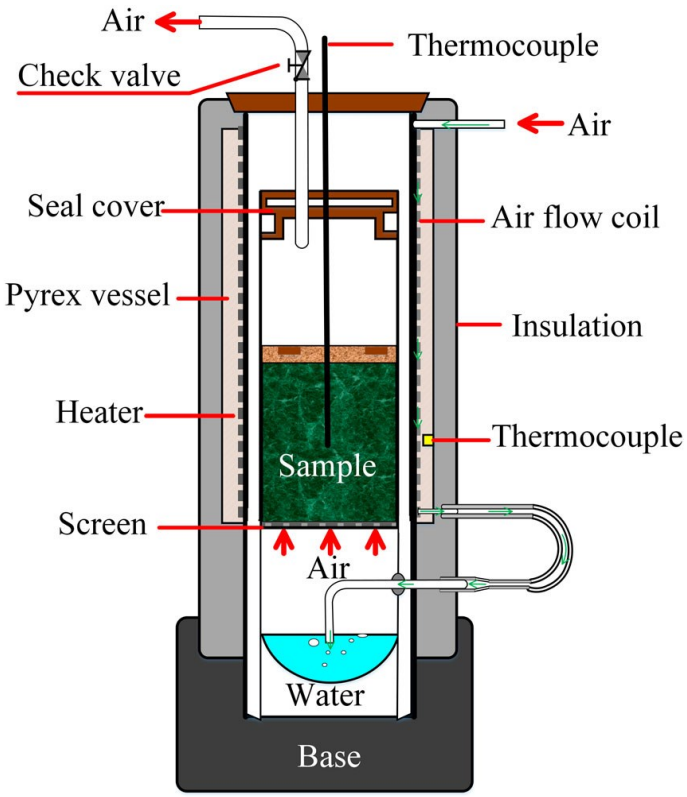

Figure A2. FR test apparatus. Adapted from (Rosenblum et al., 2001)

For each test, the temperature was raised to 140ºC under nitrogen once the 250g conditioned samples were placed in the 2L Pyrex Vessel. Then, the temperature is kept at 140ºC, and the air is introduced at 100 ml/min for 15 minutes every 5 hours for a total of 50 hours (10 cycles). The temperature is allowed to return to its baseline between each air injections. The thermogram that measures the temperature change over time is recorded, and if the sample is reactive, the Self-Heating Rate (SHR) of the sample was calculated from the temperature peaks from each air injections. With SHR, the Self-Heating Capacity (SHC) of the active sample was calculated with the following equation:

$$SHC_i = \sum SHR_i * Cp * t \quad (1)$$

Where:

SHC = Self-Heating Capacity

SHR = Self-Heating Rate

Cp = Specific Heat Capacity

T = Conditioning time (0.25hr)

Rosenblum & Spira (1995) discovered that Cps for many sulphides lie between 0.5 and 0.7 J/ g°C over a temperature range of 25 °C to 500 °C, therefore a universal value of 0.6 J/ g°C was adopted.

Therefore, Equation 1 was simplified:

$$SHC_i = \sum SHR_i * 0.15 \quad (2)$$

Units:

$$SHC_i = \sum SHR\left(\frac{^\circ C}{hr}\right)_i * 0.15\left(\frac{J*hr}{g*^\circ C}\right) = \left(\frac{J}{g}\right) \quad (3)$$

Design parameters

Table A1. Design parameters and their levels

Factors	Symbol	Coded Variable level				
		Lower	Low	Center	High	Highest
		-β	-1	0	1	+β
Time (hr)	x1	0	4	8	12	16
Temp (ºC)	x2	39	59	77	96	115
Air (ml/min)	x3	0	25	50	75	100
Moisture (wt.%)	x4	2	4	6	8	10
Sulphur (wt.%)	x5	0	2.5	5	7.5	10

approximated by the following model:

$$Y = \sum_{i=1}^{k}\sum_{j=i}^{i}\beta_{ij}X_iX_j + \sum_{i=i}^{k}\beta_iX_i + \varepsilon \quad (4)$$

where i = 5

Stage B SHCs.

Table A2. DOE results

Run	Time (hr)	Temp (C)	Air (ml/min)	Moisture (%)	Sulphur (%)	SHC (J/g)
1	12	96	25	4	7.5	4.4
2	4	96	25	8	7.5	12.4
3	8	77	50	6	5	19.8
4	4	58	75	8	7.5	8.9
5	12	58	75	8	2.5	15.4
6	16	77	50	6	5	10.9
7	8	77	50	6	10	8.4
8	8	77	50	6	5	19.5
9	8	77	50	6	0	5.5
10	4	96	75	8	2.5	26.5
11	12	96	75	8	7.5	11.3
12	12	58	25	8	7.5	8.2
13	8	77	50	10	5	32.6
14	8	77	50	2	5	4.4
15	12	96	75	4	2.5	10.6
16	8	77	50	6	5	20
17	8	77	50	6	5	21
18	0	77	50	6	5	1.5
19	4	96	25	4	2.5	8.76
20	12	96	25	8	2.5	17.6
21	8	39	50	6	5	5.5
22	4	58	25	8	2.5	5
23	4	58	25	4	7.5	10.3
24	8	77	0	6	5	1
25	8	77	50	6	5	20
26	8	115	50	6	5	9
27	8	77	50	6	5	20
28	12	58	75	4	7.5	2
29	4	96	75	4	7.5	2
30	12	58	25	4	2.5	23
31	8	77	100	6	5	11
32	4	58	75	4	2.5	4

Simplified ANOVA table

Table A3. Simplified ANOVA table for the regression model

p-value	F-value	R^2 (%)	S
0.048	2.68	82.95	5.56

Residuals

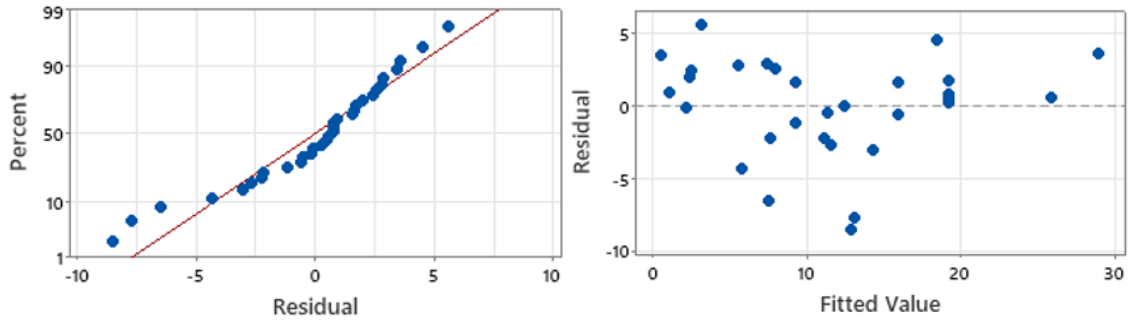

a) b)

Figure A3. a) Normal probability plot and b) Residual plot

Residuals shown in Figure B-1 a) generally lie on a straight line, meaning that errors are distributed normally. Figure B-1 b) shows that the residuals scatter randomly, suggesting model predictions are adequate.

Student's T test.

Table A4. Student's t-test data

Term	T-Value	*P*-Value
Time (hr)	1.23	0.245
Temp (C)	0.87	0.402
Air (mL)	0.41	0.693
Moisture (%)	3.55	0.005
Sulphur (%)	-1.67	0.123
Time (hr)*Time (hr)	-2.59	0.025
Temp (C)*Temp (C)	-2.33	0.040
Air (mL)*Air (mL)	-2.63	0.023
Moisture (%) *Moisture (%)	0.41	0.691
Sulphur (%) *Sulphur (%)	-2.40	0.035
Time (hr)*Temp (C)	-1.18	0.265
Time (hr)*Air (mL)	-0.85	0.415
Time (hr)*Moisture (%)	-0.68	0.508
Time (hr)* Sulphur (%)	-1.35	0.204
Temp (C)*Air (mL)	1.05	0.315
Temp (C)*Moisture (%)	1.97	0.075
Temp (C)*Sulphur (%)	-0.69	0.504
Air (mL)*Moisture (%)	2.10	0.059
Air (mL)*Sulphur (%)	-0.59	0.564
Moisture (%) *Sulphur (%)	0.18	0.862

Main effects for SHC

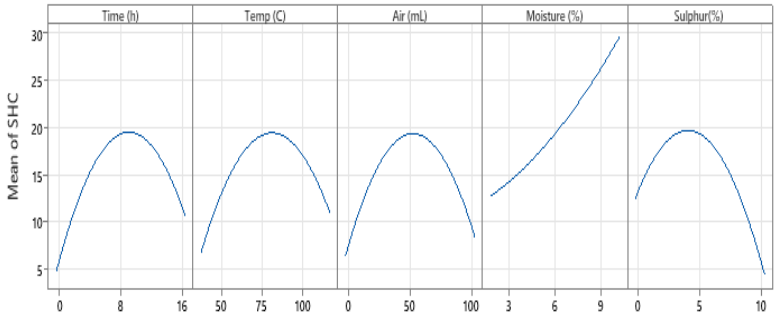

Figure A4. Main effects plot for SHC

Optimum Conditions

Table A5. Optimum conditions

Variables	Units	Variable ranges for high SHC	Supporting graphs
Time	(hr)	3.8-12.7	Figure A-5 (a – d)
Temperature	(ºC)	80-115	Figure A-5 (a, e, f, g)
Air	(ml/min)	9.2-10	Figure A-5 (b, e, h)
Moisture	(wt.%)	55-88	Figure A-5 (c, f, h, j)
Sulphur	(wt.%)	1.2-7.5	Figure A-5 (d, g, i, j)

Validation test parameters

Table A6. Optimum condition and validation test results

Validation test no.	Time (hr)	Temperature (°C)	Air (ml/min)	Moisture (wt.%)	Sulphur (wt.%)	SHC (J/g)	SHC calc	Error (%)
1	7	80	70	10	4	36	34	6
2	8.5	95	80	10	3	42	39	7
3	8	90	60	10	4	34	35	3
4	8	85	60	10	3	34	33	3

Optimum condition thermograph.

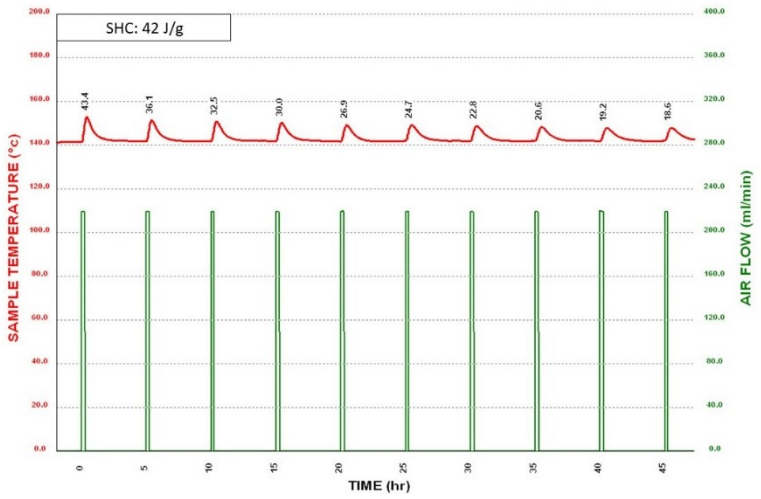

Figure A5. Stage B thermograph of validation test no. 2

Rosenblum, F., Nesset, J., Spira, P., Evaluation and control of self-heating in sulphide concentrates. CIM bulletin, 2001, 94(1056**)**, 92-99.